ADDIS ABABA UNIVERSITY

ADDIS ABABA INSTITUTE OF TECHNOLOGY

SCHOOL OF CIVIL AND ENVIRONMENTAL ENGINEERING

RUNOFF AND SEDIMENT YIELD ESTIMATION UNDER LAND USE LAND COVER DYNAMICS (A CASE STUDY OF GENALE DAWA DAM-3)

A THESIS IN HYDRAULIC ENGINEERING STREAM

BY

GIRMA SOLOMON KASSAYE

ADDIS ABABA

September, 2020

A THESIS

SUBMITTED IN PARTIAL FULFILLMENT OF REQUIREMENT FOR THE DEGREE OF MASTER SCIENCE

Approval page

The undersigned have examined the thesis entitled '**runoff and sediment yield estimation under land use land cover dynamics (a case study of Genale Dawa Dam-3)**' presented by **Girma Solomon**, a candidate for the degree of **Master of Science** and herby certify that it is worthy of acceptance.

---	---	---
Advisor	Signature	Date
---	---	---
Internal examiners	Signature	Date
---	---	---
External examiner	Signature	Date
---	---	---
Chairman	Signature	Date

Undertaking

I certify that research work runoff and sediment yield estimation under land use land cover dynamics (a case study of Genale Dawa Dam-3) is my own work and work has not been presented elsewhere for assessment. Where material has been used from other source it has been properly acknowledged/referred.

Signature _____

Girma Solomon

ACKNOWLEDGMENTS

First of all, I would like to thank the almighty God for his never ending gift and his provision to complete this work.

I would like to express my sincere appreciation to my Advisor Dr. Daneal Fekreselassie for the devotion of his precious time to valuable suggestion, guide, and comment of my work. I am also grateful to my friends for all challenges and knowledge sharing.

ABSTRACT

The study of stream flow patterns with respect to LULC changes helps the assessment of sustainability of land use/cover systems. The dynamics of Land use/cover is one of the causing factor to change the hydrologic response of the Ganale sub-basin resulting for soil erosion and over producing of runoff and sediment yield. Therefore this thesis is attempted to access the effects of land use/cover changes on Genale Dawa Dam-3 reservoir sedimentation for the year of 1994, 2000, and 2017.

The land use/cover was generated from satellite image using ERDAS Imagine 2014 software. Using the three land use/cover and the same other input data (DEM, climate data and soil map) for all, three independent model were delineated. The delineated Genale sub-basin was divided into 286 sub-basins and 2632 HRU's for 1994 and 2000, 2449 HRU for 2017. Model calibration and validation was done successfully at Chenemesa gauging station. Calibration and validation of the SWAT model was done under sensitivity analysis by means of using SWAT-CUP software SUFI2 program. Hence calibration and validation of flow and sediment yield for each model is conducted from 1990-2005 and 2006-2015 respectively.

Accordingly the R^2 and NSE were found to be in the acceptable range (0.66 to 0.71 for R^2 and 0.51 to 0.65 for NSE). The evaluation of land use/cover result showed that the average annual Sediment load and runoff at upper Genale Dam-3 site is found that 14.1 ton per ha per year, 77.8mm for land use/cover in 1994 was 16.4 ton per ha/year, 102.2mm for land use/cover in 2000 and 24.3 ton per ha per year, 130.6mm for land use/cover in 2017 respectively. Variability of sediment yield in Genale sub basin are fluctuates between 0.1ton per ha per year to 129 ton/ha/yr. in 1994 of LULC, 0.1ton/ha/yr. up to 111 ton/ha/yr. in 2000 LULC and 1 per ha per year to 162 1ton per ha per year in 2017LULC in annually average during the period from (1990-2017) respectively. The model prediction results indicated that in 1994, 2000, and 6.7%, 5.2%, and 11.9% of Genale sub-basin area were highly eroded by producing greater than 50 ton/ha/yr.

Therefore, the result of the study shall be supports different concerned party to plan and implement suitable soil and water conservation approaches.

Key word: Genale sub-basin, land use/cover change, runoff, sediment yield, SWAT model, ERDAS, SWAT-CUP, calibration, validation, streamflow.

Table of Contents

List of Tables

List of Figure

LIST OF ABBREVIATION

A.S.L	above sea level
Arc SWAT	ArcGIS Interface for Soil and Water Assessment Tool
DEM	Digital Elevation Model
ERDAS	Earth Resource Development Assessment system
ETM+	Enhance Thematic Mapper Plus
FAO	Food and Agricultural Organization
GDMP	Ganale Dawa master plan
GIS	Geographic Information System
HEC-HMS	Hydraulic Engineering Center-Hydrologic Model Center
HRU	Hydrologic Response Unit
LULC	Land use land cover
LULCC	Land use land cover change
MoWIE	Ministry of Water Irrigation and Energy
NDVI	normalized difference vegetation index
NSE	Nash and Sutcliffe Efficiency
R2	Coefficient of determination
SUFI2	Sequential Uncertainty Fittings 2
SWAT	Soil and Water Assessment Tool
SWAT-CUP	Soil and Water Assessment Tool-Calibration and Uncertainty
TM	Thematic Mapper

USA	United States of America
USDA- SCS	United States Department of Agriculture
USGS	United States geological survey
USLE	Universal Soil Loss Equation
WAPCOS	water and power consultancy service
WXGEN	Weather Generator

CHAPTER ONE

1. INTRODUCTION

1.1. Background

Soil erosion is a composite land degradation process which leads the soil to decrease in quality and productivity and results the decreasing in infiltration and escalation in runoff (Gemechu 2014).

Land cover changes may have instant and long-term impacts on terrestrial hydrology and, change the long term balance between rainfall and evapotranspiration and the resulting runoff. In the short-term, destructive land use dynamics may disturb the hydrological cycle either through increasing the water yield or through decreasing, or even eliminating the low flow in certain circumstances (Croke, Merritt, and Jakeman 2004).

The study of stream flow patterns with respect to LULC changes helps the valuation of sustainability of land use/cover systems; because stream flows reflect on the hydrological system of the entire watershed. As different researchers indicated, the hydrological outcome of land use/cover changes is a referencing issue and much research is essential.

The appropriate tools are necessary for better assessment of long-term hydrological as well as soil erosion processes and as decision support for planning and performing suitable measures. These tools include various soil erosion and hydrological models, along with geographical information system (GIS). Thanks to the technology advances in the recent time, the distributed sub-basin models are widely used to implement alternative management approaches in the water resources allocation and flood control (Shimelis G. Setegn, 1, 2* Ragahavan Srinivasan 2010). Different hydrological models were designed to delineate soil erosion or sediment yield and hydrological processes. Hydrological models define the physical processes governing the transformation of precipitation to runoff, whereas modeling of soil erosion defines the understanding of the processes of physical laws that happen in the natural landscapes (Shimelis G. Setegn, 1, 2* Ragahavan Srinivasan 2010).

Therefore, the target of this research is applying the combination of GIS and (ERDAS imagine 2014 software) and physically based semi distributed model (SWAT), to realize the influences of LULC changes on runoff and sediment yield of Genale sub-basins.

1.2. Statement of problem

Understanding the hydrological processes is the important point for good managements of water and land use/cover resources. The change of land use/cover may lead to considerable changes in evapotranspiration, leaf area index, infiltration rates, soil moisture content, surface roughness, sub-surface flow regimes, surface runoff, and soil erosion through interactions with vegetation, soils, topography, geology and climate processes.

The need of land for cultivation is growing from time to time and leads to deforestation from the day to day activities of the people living in the Genale sub-basin. As a result the Genale sub-basins are highly exposed to high soil erosion by the impacts of severe rainfall that may be the causes for increasing of land use/cover dynamics which results the generation of runoff in the Genale sub-basin. This continuous change of land cover has affected the runoff and sediment yield of the Genale sub-basin by varying the amount and the components of stream flow which causes surface runoff and sediment yield transport, and which rates the increasing of reservoirs sedimentation problem.

The speedy of land use/cover alterations caused by removal of a forest for cultivation purpose are assumed to adversely affect the runoff and sediment of the Genale Dawa-3 reservoir. In addition spatial variability in soil erosion and siltation has also happened in the sub-basin. Hence, the careful requirements of identification for a hydrological methods and tools that would be estimate the impact of land cover alterations on the runoff and sediment yield of the sub-basin. Such methods or tools can deliver the information that shall be used for water resources management at the given sub-basin.

1.3. Objective of the study

The general objective of this research is to access the amount of runoff and sediment yield under land use land cover dynamics that comes from Genale sub-basins into Genale Dawa Dam-3 reservoir.

1.3.1. Specific objective

- To analyze the LULC changes over the period of the three years (1994, 2000 and 2017).
- To identify the flow and sediment sensitive parameters of the watershed
- To compute the effects of LULC changes on the runoff and sediment yield of the Genale sub-basin at the dam three reservoir site.
- Assess and evaluate the spatial variability of sediment yield in the sub-basin and identify high erosion yielding areas in the sub-basin.

1.4. Research question

- How to compute the effect of LULC changes over a three base periods (1994, 2000 and 2017)?
- What are the flow and sediment sensitive parameters of Genale sub-basin?
- How much amount of sediment is coming to the reservoir per year from the Ganale River?

CHAPTER TWO

2. LITERATURE REVIEW

2.1. Concept of land use land covers changes

Land cover is the physical characteristics or state of Earth's surface, having the distribution of vegetation, water, bare soil and artificial structures. Land use refers to the future use or management of land cover type by human existences such as farming or cultivation, forestry and building construction. Land use land cover changes are generally classified into two main types: conversion (change from one use or cover types to another e.g. from forest to grass land) and modification (a modification within one LULC kind for instance from rain fed cultivated area to irrigated cultivated area) (McNeil et al. 1994).

LULCC is usually caused by several interacting factors initiating from different level of organization of coupled human environment systems. It is the consequence of composite interfaces between numerous biophysical and socio-economic circumstances which may happen at several temporal and spatial levels. The combination of driving forces of LULCC fluctuates in time and space according to specific human-environment situations. Understanding the underlying LULCC drivers are an important input for planning and decision making (Xiuwan 2002).

The study of LULCC is frequently necessitated by the need to know, in quantitative terms, nature, extent and the rate at which these changes advance and the problems or influences they cause. In addition, some studies are tried to realize the effect of changes in upstream land use and land cover, causing an alterations in the movement of water and water availability at the downstream. The Improved realization of these impacts enhanced their estimating, forecasting and modeling at a regional scale. But, computing the impacts of LULCC and managements practices at the sub-basin level is still complex because of the complex and variability of characteristic interactions among the different factors. Therefore, in order to provide the foundations for the effective management of the natural resources, an understanding on the variability in time and space should be built up for the resources and role of human cultures and institutions in bringing those variations(Klein Goldewijk and Ramankutty 2004).

Collective knowledge of LULCC is helpful to reconstruct the past land use and land cover changes and to predict future changes, and hence this may help in elaborating sustainable management practices aimed to maintaining essential landscape functions (Hietel, Waldhardt, and Otte 2004). The main cause of LULCC and their relationship with the hydrological regimes must to be identified to develop the forecasting of the future land use and management decision results under the range of economic, environmental, and social scenarios.

At this time, the enhanced consideration of the processes of LULCC has run to a change from a view condemning human impact on the environment as leading mostly to the deterioration of the earth system processes to emphasis on the potential for efficient exploitation of resources and ecological restoration by managing a watershed. such change of LULC may reflects to raise the research questions, methods, and scientific paradigm(Victor and Ausubel 2000). Consequently, the general avowals about the impacts of LULCC and land water relations requires the continuous question to decide whether they represent the best available information or not (Woldeamlak Bewket and Sterk 2005).

2.1.1. Land Use and Land Cover Change Studies in Ethiopia

In Ethiopia most of the land use is at the hand of few farmer who work for survival. With the high population growth and low rate of agricultural escalation, few farmers require extra land to grow crops for survival. This will results in deforestation and land use transformation from other types of land cover to cropland.

Different researchers have been showed that there were a significant land use and land cover dynamics in different parts of Ethiopia. Many of these research shows that croplands have been increased at the spread of natural vegetation comprising forests and shrub lands; such as (Belay, 2002); (W Bewket 2003); (Abebe, 2005) in northern part of Ethiopia, (Zeleke and Hurni, 2001) in north western part of Ethiopia, (Kassa, 2003) in north eastern part of Ethiopia; and (Denboba, 2005) in south western part of Ethiopia.

Kassa (2003) in his research, around southern Wello, he described that the decreasing of natural forests and increasing of grazing lands due to conversions to agricultural lands. Bewket (2003) have also stated that there was an increasing of wood lots (eucalyptus tree plantations) and agricultural land at the expenditure of grazing land in both Chemoga watershed in north-western

Ethiopia, and Sebat-bet Gurage land in south-central Ethiopian. In addition Gebrhiwet also describes that the dynamics of land use and land cover that happened from 1971/72 to 2000 in Yerer Mountain and its neighboring results a growth of farming land at the expenditure of the grasslands (Gebrehiwet, 2004).

(Hadgu, 2008) also recognized that there were a reduction of natural vegetation and growth of agricultural land over the period of 41 years in Tigray, northern part of Ethiopia. He decided that the population growth was an important factor for the increasing and strengthening of agricultural land in recent periods. (Garedew, 2010) stated that throughout the period of 1973-2000 in the semiarid areas of the central Rift Valley of Ethiopia, cropland coverage has been expanded and woodland cover were decreased. The study conducted on a Hare watershed, in Rift Valley of Ethiopia, Kassa, (2009) shows that because of the replacement of natural forest by farmland and settlements, the mean monthly discharge for wet months had been increased whereas in the dry season reduced.

As different literatures result shows that the population growth has a very high impact on the environment. For example, according to Tekle and Hedlund, population growth has been start to have side effect on Riverine vegetation, scrublands and forests in Kalu district (Tekle and Hedlund, 2000), Riverine trees in Chemoga watershed (Bewket, 2003), and also the natural forest cover in Dembecha Woreda north-western Ethiopia (Zeleke and Hurni, 2001).

2.1.2. Land Use and Land Cover of Genale Dawa basin

In Ethiopia Land use is highly affected by landform, climate, and socio-economic features. So Genale dawa basin is one of the basin found in Ethiopia which contains with an enormous diversity of natural and manmade landscapes, through the elevations ranging varies from 180masl to over 4000masl, covering of different climate zones. It is possible to say all of the Ethiopian's agro-economic zones and all major land use system of the country were found within this basin (GDMP 2007).

As the result of different study's shows the distribution of land cover classes and land use maps shows the predominance of grassland and bush land was found within the basin. Majorly these land cover types are found in the hotter and dryer lowland areas. Cultivated land covers for about 16% of the basin area which is parallel to the national average of 15%. The significant area

(66%) within the basin is cover by grassland and bush land in that way it was a good providing of a vital resource for an enormous livestock population. Settlements, afro-alpine and sub- afro-alpine vegetation, and water bodies covers very small proportion (2%) of the basin, but then again the degraded and the exposed surface area which is not exploited is now more than 6%(GDMP 2007).

Land use variations that has been taken place within the basin during the past 12 years are because of the needs of population primarily increasing for food production and again to substitute the degraded natural forest areas in the upper wurch (>3200m), lower wurch (2701-3200m) and Dega(2401-2700) elevation areas.

Land use changes that happened in the Genale Dawa basin are:

1. Ensuing the croplands for at least 5 years period for grazing and regeneration of fertility

2. Changing of mixed high forest, wooded bush land, woodland, grassland and bush lands to cultivated rain fed and irrigated fields, and

3. Enhancement of natural vegetation areas for starting new croplands (GDMP 2007).

2.2. Image Classification

Image classification is practically the best significant part of digital image analysis. It is very good to have an "interesting picture" or images that representing the extent of colors showing various features of the underlying terrain. However, it has no benefits without identifying what is the meaning of colors. The classification of Image is used to detect and describe, as a unique gray level (or color), the features occurring in an image in terms of the thing or type of land cover these features really represent on the ground. Image classification process is required for classifying all pixels in the form of digital image into several land cover classes, or "themes". To create thematic maps present in image of the land use land cover the classified data may then be used. Actually, for the numerical beginning for categorization multispectral data are used to accomplish the grouping and the spectral patterns existing within the data for each pixel (Ahmed 2006)

For the ultimate thoughtful of remote sensing and digital images through the major stages the processing of image was taken place. For the application of image processing and to introduce a wide range of processing techniques it provides a varied set of the cases. This formulates the basis for continued progresses to the advanced level. It was the procedure of assigning each pixel of an image to a particular group or class.

Therefore this is not only the case that the classes are land cover or crop types; it is also to map the land cover types of the whole image. Commonly these were acquiring the ground reference land cover information from a field site data within the image.

Supervised classification and unsupervised classification are two main classification methods. Image classification is mostly performed using ERDAS Imagine software. An image processing software package that allows users to process the geospatial and other imagery as well as vector data is ERDAS Imagine. In addition the ERDAS image can handle hyper spectral imagery and LiDAR (Light Detection and Ranging) from various sensors. And also it compromises a 3D viewing module (Virtual GIS) and a vector module for modeling. The native programming language is known as EML (ERDAS Macro Language). ERDAS is integrated with the other application such as GIS and remote sensing applications and the storage format for the imagery can be read in many other forms of applications (*.img files)(Ahmed 2006).

A. Supervised Classification

The classifier/expertise identifies the samples of the info of land use or cover classes of the concerned image during supervised classification, which is known as "training sites". To change the statistical characterization of the reflectance for every info class image processing software system was used. The step was commonly known as "signature analysis" and it consist of the changing of characterization as simplicity of the normal reflectance on each bands, or as complication of the mean, variances and covariance over very bands. After a statistical characterization has been completed for each information class, the image is then classified by inspecting the reflectance for each pixel and making a decision about which of the signatures it look like utmost (Ahmed 2006).

The objective of this procedure is to broaden, or extrapolate information on land cover types from a identified area of the image to the unidentified areas of the entire image. The image analyst describes number of training areas for each land cover classes.

Depend on this information the ERDAS 2014 imagine generates spectral signatures. To measure the spread of values around the mean of the class typically a maximum likelihood descriptor is used. Each pixel of the image is assigned to some of the land cover groups, as defined by the signature (Ahmed 2006).

B. Unsupervised Classification

Unsupervised classification is the technique that inspects an enormous amount of unidentified pixels and splits into small classes depend on the natural groups found in the image. Unsupervised classification do not need of analyst-specified training data like supervised classification. This classification system is the automatic classification by the erdas 2014 software which classifies in to different categories of similar gray level. Therefore, somewhat unsupervised classification was the easiest method. For the given image data the computer is requested to decide a user-defined number of clusters for the different wavelengths. Every cluster represents the land use/cover classification. The average digital value for every input band was indicated by the spectral reflectance profile. The spread of values around the average for the LULC classification represents by the cluster. Then after the classification has been accomplished every class would be examined and assigned a name. It can be also essential to combine certain classes into a single category (Ahmed 2006).

The classification outcomes of the unsupervised classification is depend on natural grouping of image values, and the identification of these spectral classes is initially not known, and therefore it should be compared with the classified data of other referenced data (such as imagery map, or site visits) to decide the character and informational values of the spectral classes(Abby et al. 1997).

An unsupervised classification method has more advantages where there is no ground information data exists; is not biased in defining classes; is comparatively fast to compute; and considering for all cover types in an image. Therefore the process of categorizing and merging

classes cannot time taking and the statistical description of the spread of values within the cluster is not the same as the maximum likelihood classifier.

In opposition the supervised maximum likelihood approach is time consuming when identifying training areas; relatively slow to compute; and can only produce a class map for which there are training areas(Lemenkova 2015).

Unsupervised classification is now a day becoming widely held in agencies included in long term GIS database maintenance. The reason is that there are now systems that use clustering procedures that are very fast and needs little in the nature of operational parameters. Thus it is becoming possible to train GIS analysis with only a general familiarity with remote sensing to undertake classifications that meet typical map with the accuracy standards. With the suitable ground truth accuracy assessment procedures, the tool can provide remarkably fast and good quality of land cover data on a continuing basis (Ahmed 2006).

2.3. `Sensitivity Analysis

Sensitivity analysis is the way of finding of the model parameters that has high effects on model calibration (on model predictions). The model sensitivity analysis explains that in what manner model output varies from the given input data. Regarding to this case (Lenhart 2002) reviewed more than a dozen sensitivity analysis techniques. In general the important objective of this parameter sensitivity analysis is helpful for reducing the number of parameters that must be estimated to reduce the work out time necessary for model calibration.

The SWAT simulation is gone on when there will be a disagreement among the observed data and the simulation outcomes. Thus, to diminish this deviation, it is very essential for determining the parameters that may influence the outcomes and the degree of deviation. Therefore to check out the deviation, sensitivity analysis is done by SWAT-CUP 2012 software to express the rank of sensitivity of parameters to put the degree of sensitivity in order. This significantly simplifies the total calibration and validation progresses and decreasing the time required for calibration. The method that are applied for sensitivity analysis is done by using SWAT-CUP which is called the Global sensitivity analysis design according to (Morris and Fan 2000).

2.4. Related previous works by SWAT

SWAT is one of the most commonly used model and scientifically recognized tools for the valuation of water quality, sediment transport and stream flow in a watershed. For these cases there are different reports as evidenced in worldwide Conferences and publications of SWAT. The primary use of the model is driven by the demand of several environmental agencies for straight and exploratory assessments of the impact of anthropogenic activities, climate change and extra wide range of land management issues on water and soil resources (Gassman and Reyes 2016).

In the Upper blue Nile Basin in east Africa, SWAT has been used for hydrology/water balance, erosion, water quality, and climate change assessments, calibration uncertainty, land use change researches, and SWAT development(Zheng et al. 2012). Moreover, (Gassman et al. 2007) also showed that there are global application of SWAT involved calibration and/or sensitivity analysis, climate change impacts, GIS interface descriptions, hydrologic assessments, variation in configuration or data input effects, comparison with other models or techniques, interfaces with other models, and pollutant assessments.

The calibration and validation by the SWAT model application was done in most of Ethiopian areas (Shimelis G. Setegn, 1, 2* Ragahavan Srinivasan 2010);(Woldeamlak Bewket and Sterk 2005); (Tesfahunegn, Vlek, and Tamene 2012) have already shown that SWAT model was evaluated with adequate level of accuracy in gauged catchments in some parts of Ethiopia.

CHAPTER THREE

3. MATERIAL AND METHODS

3.1. Description of the Study Area

3.1.1. Locations

Genale-Dawa River is a long river in the northeast of Africa which is originating from the south of Songkalu Mountain in the south part of Ethiopia. The upper reach of this river is called Genale River, which flows southeast ward to the boundary of Ethiopia and Somalia, Dolo where it joins Dawa River and Welmel River and it is then after called Juba River. The Genale sub-basin or the study area is found at the upper part of Genale river which is located between longitude 38°30′-42°20′east and latitude 4°14′~7°05′north, the Genale sub-basin River has a full length of about 2382.080 km and a basin area of 55,754.2 km2.

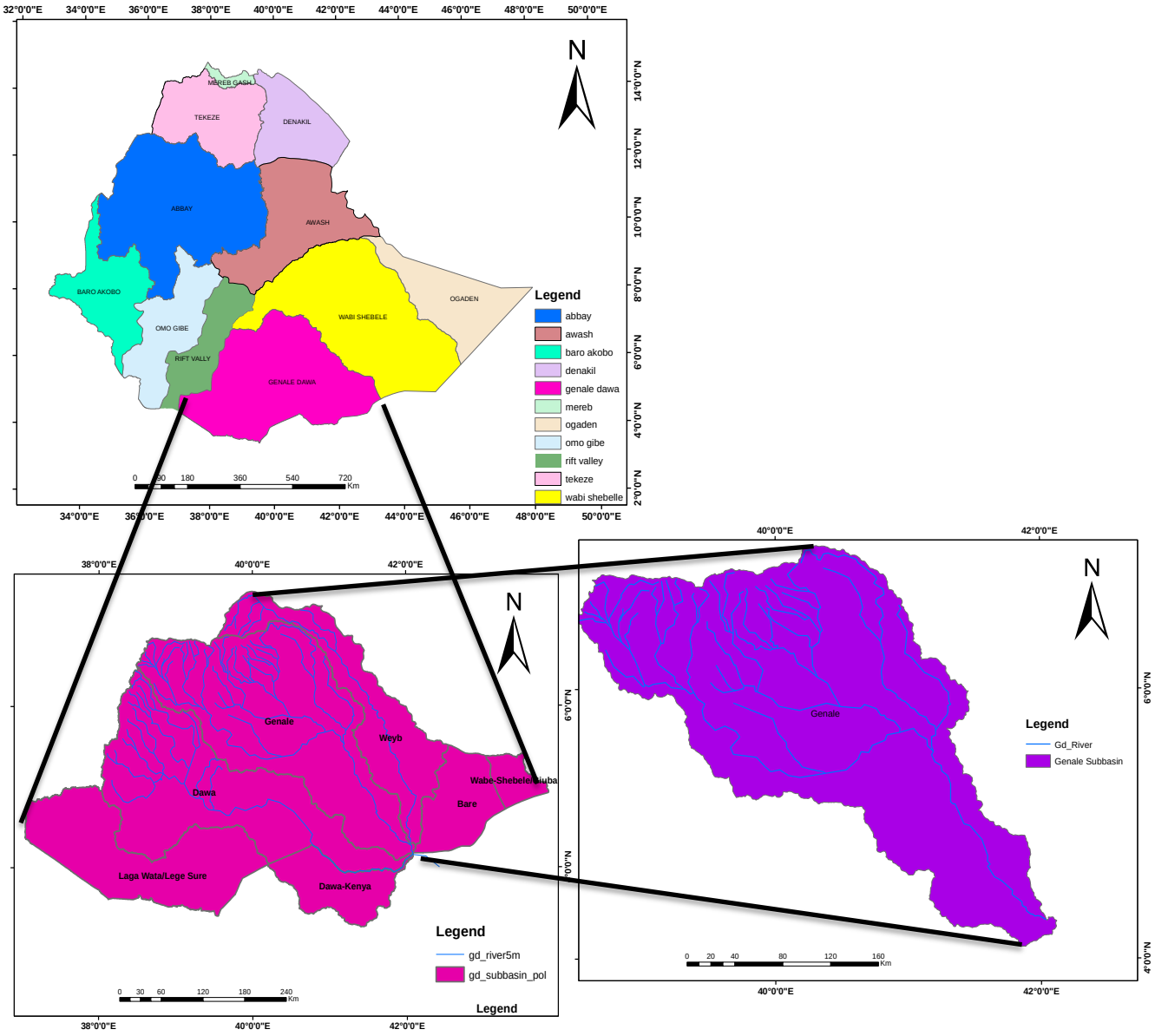

Figure 3.1 Location of Genale sub-basin

3.1.2. Topography

The diversity of geographical, topographical, and climatological features are found in Ethiopia which means from high rugged mountains to deep gorges; from lowest altitude at about 120m below sea level to highest altitude of 4600m above sea level; from 2000mm high annual rainfall to 200mm of low annual rainfall (GDMP 2007).

According to (WAPCOS, 1990) the general physiographic features of the Genale-Dawa River Basin have been defined in terms of four major landforms as cited in (GDMP 2007).

- Steep sloping escarpments
- Gently sloping lowlands adjacent to the foot of the escarpments
- Lowlands and
- flood plain basins

The main river drainage system is defined by three principal tributaries in the upper section: Upper Genale, Geberticha and Iya. These tributaries originate from the Sidamo Mountains which form the watershed-divide between Genale and the neighboring Rift Valley and Wabe Shebelle river basins. The highest point on the northern divide is Mount Korduro with elevation around 3,750m a.s.l. Other mountain peaks with elevations exceeding 3,000 m a.s.l. can be found in this area (GDMP 2007).

3.1.3. Climatic features

Climate is one of main factor that influenced by the effects of elevation, which gives rise to distinct zones and characteristics. The common known traditional classifications of climate based on altitude and temperature which are predominant in the Genale Dawa river basin are;

- **Kola**: - tropical hot and arid type, below 1500 m altitude with mean temperature in the range 20-28 ºC.
- **Woine Dega**: - sub-tropical warm, between 1500-2500 m altitude with mean temperature in the range 16-20 ºC.
- **Dega**: - temperate highland climate above 2500 m altitude with mean temperature in the range 6-16 ºC. (GDMP 2007).

The easterly and southeasterly moist air currents ascend over the highlands in spring, produce the main rainy season in southeastern Ethiopia in general, and in Genale Dawa basin in particular

and bring small rains of spring (March to May) to most parts of the country. Southeast (Genale Dawa river basin), therefore, gets its first maxima rainfall during spring and receives the year's secondary maxima rainfall during autumn from the Indian Ocean easterlies as shown in figure 2.2. While the basin receives little rainfall in summer compared to spring (March to May) and autumn (September to November) due to the case that the Southerly Indian Ocean air currents lie in the lee side of the highlands in summer and Atlantic westerly reach the southeastern lowlands Ganale Dawa after losing their moisture on the highlands to west (Asmerom 2015).

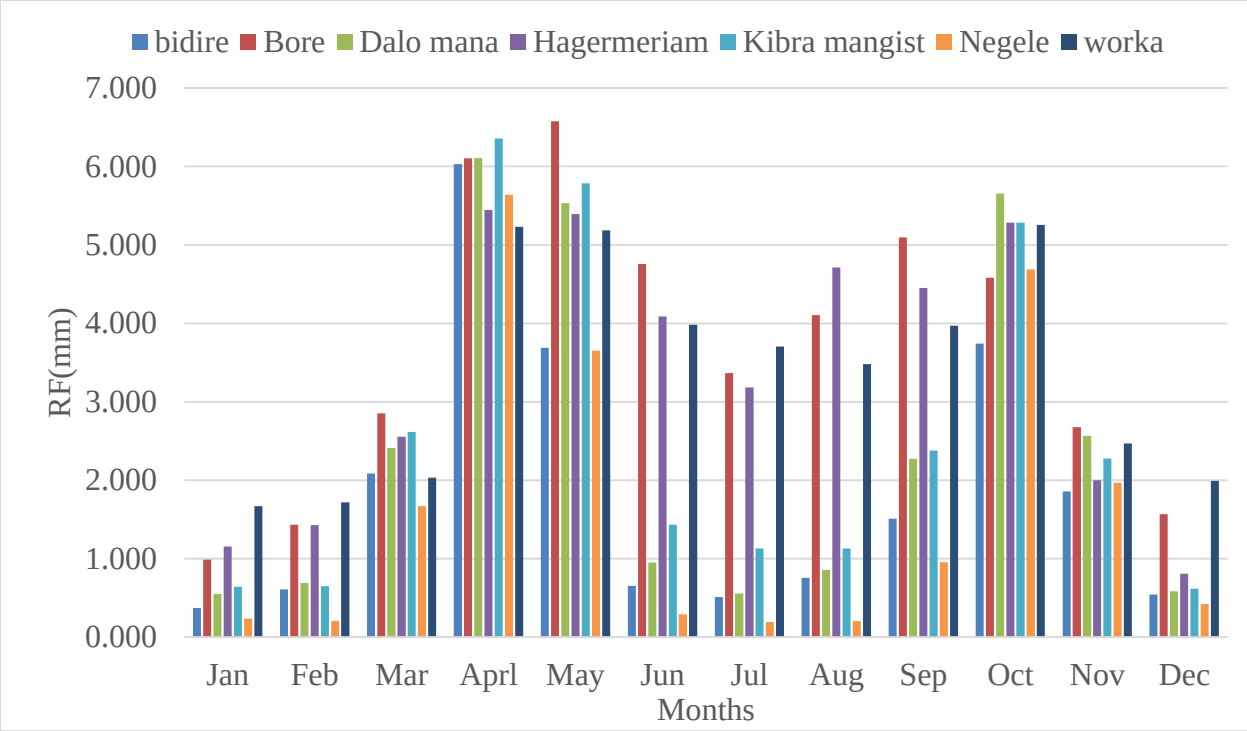

Figure 3.2. The average monthly rainfall of Ganale sub-basin

3.2. Materials and data needed

To carry out this study the following materials and data was acquired for data processing and evaluation.

- The historical flow data, sediment data, soil data and climate data are collected from ministry of water electric and irrigation and national metrological agency respectively.
- DEM and land use land cover data of three Landsat images are downloaded from USGS.
- Arc GIS (software) - which is a tools used in this study for projection and processing of DEM, watershed delineation, land sat image and stream flow determination.
- ERDAS-2014- used to classify land use/cover by layer stacking, mosaic, and classification by unsupervised classification with the combination of google earth pro.
- Arc SWAT (model) – is one of the tools which were used in this study for model calibration and validation in the catchments. This model enables to predict annual runoff and sediment yield enters into the reservoir and its distribution in each sub-basin.

3.3. Methodology

The methodology of this study has been done by following procedures.

- Data collection (secondary data)
- Data analysis
- Data input and processing
- Model setup and simulation
- Model calibration and validation
- Runoff and sediment yield modelling
- Output data interpretation
- And again by changing only land use/cover follow the same step and then calibrate and validate the model for three LULC, finally compared and analysis the result.
- From the model simulation result, the sediment source area will be identified by classifying into sub-basin by categorizing sediment load or erosion low, medium, high and very soil erosion condition.

3.3.1. Data collection and analysis

Metrological data, hydrological data, topographic and land use data was the basic data sets required to develop input for SWAT model. SWAT model largely depends on hydro-metrological data such as stream flow, sediment, precipitation, temperatures, wind speed, relative humidity, and solar radiation.

3.3.1.1. Metrological data

The input data needed by SWAT model includes daily data of weather condition which was gathered from national metrological agency (from observed data). The seven meteorological stations which have reliable recorded data are presented in (Table 4.1) which is within and around the sub-basin.

Table 3.2-1 Metrological station in and around Ganale sub-basin

SNo	Station name	Lat.	Long	Elev.	Rainfall	Temp	Sunsh.	Hum	Win
1	Bidere	39.62	5.77	1400	✓	✓	NA	NA	✓
2	Bore	38.62	6.35	2712	✓	✓	✓	✓	✓
3	Dello Mena	39.83	6.42	1313	✓	✓	✓	✓	✓
4	Hageremariam	38.52	6.49	2809	✓	✓	NA	NA	NA
5	Kibre Mengist	38.97	5.87	1680	✓	✓	✓	✓	✓
6	Negele	39.57	5.42	1544	✓	✓	✓	✓	✓
7	Worka	39.22	6.48	2450	✓	✓	✓	✓	✓

Lat= latitude, Long= longitude, Elev= elevation above mean sea level, NA=Non-available data, Temp= temperature, Sunsh= sunshine hour, Hum= humidity.

In any water resources development activities, the hydro-metrological data screening, Checking of consistency, homogeneity of data and analysis come first to check the quality of data. Therefore in this study the following techniques are used to check the quality of available data.

Homogeneity test

A time series of observational data is relatively consistent and homogeneous when a periodic data are proportional to the suitable simultaneous period. The non-dimensional rainfalls records are plotted to relate the stations with each other. Graphical comparison of the rainfall data was done by plotting the time series of monthly rainfall data. The monthly Non-dimensional values of the precipitation in each station can be computed by;

$$P_i = \frac{P_{i,avg}}{P_{avg}} * 100 \quad \text{-----------} \quad 4.1$$

Where, Pi is non-dimensional value of precipitations for a months in stations i, $P_{i,avg}$ over years averaged monthly precipitations for station i and P_{avg} is over year's averaged yearly precipitation of the station i.

The stations that used for this study were homogeneous and have a rainfall pattern of bimodal with high rainfall season as shown in the Figure (4.1).

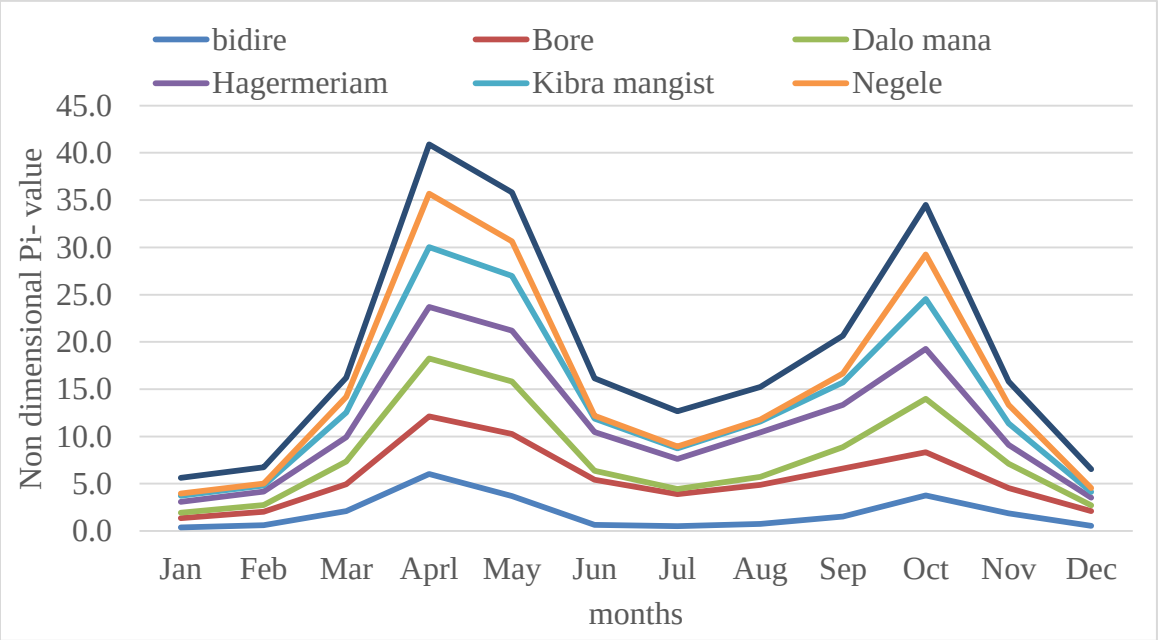

Figure 3.2. Homogeneity test for stations of study area

Checking Consistency and Adjustment of rainfall stations

A double mass curve technique was applied for checking of consistency of the selected station in sub-basin. This method is known as graphical method that is used for checking and adjusting the inconsistency of every station data by relating there trend with that of neighboring stations. This inconsistency shall be identified from the time to the substantial change happenings. In the condition where the significant change in the regime of curve is observed, the following is used for the corrected. (4.2).

$$P_{cx} = P_x \frac{M_c}{M} \quad \text{---------- 4.2}$$

Where, P_{cx} = Corrected precipitation at station X,

P_x= Original recorded precipitation at station X,

M_c = Corrected slope of the double mass curve

M = Original slope of the double mass curve.

The selected stations show similar periodic pattern of records (Figure 4.2) and stations used in this study has not a substantial change throughout the base line period (1988-2017) of the study.

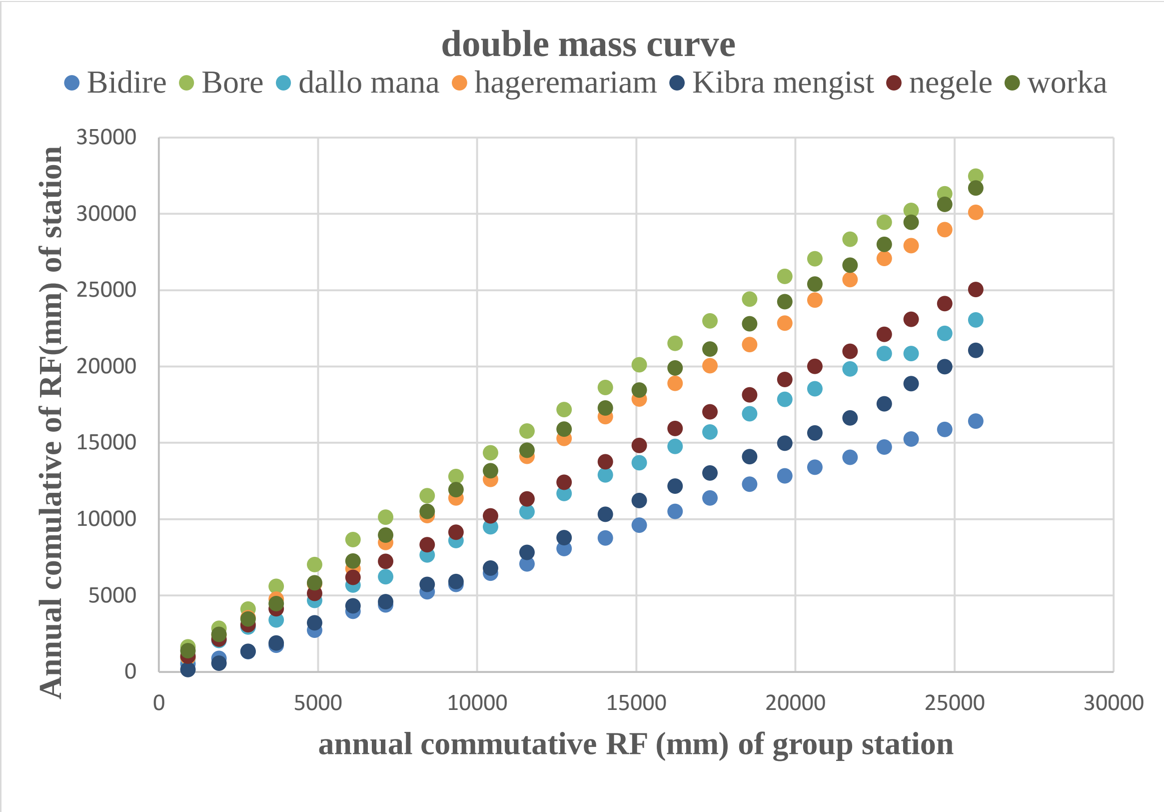

Figure 3.2 Double mass curve

Filling Missing Rainfall Data

The continuity of a record may be broken with missing data due to damage or fault of a rain gauge during a period. The missing data can be estimated by using the data of neighboring stations. Simple Arithmetic mean method were applied if the average yearly rainfall of the total index stations is within the limit 10% of the station under consideration station (x) and which is calculated by using Equation (4.3.), and while if the average yearly rainfall of the neighboring stations varies from that of station (x) by greater than 10%, normal ratio method shall be applied by using Equation (4.4).

$$P_x = \frac{1}{N} (P_A + P_B + P_C \dots \dots + P_N) \dots \dots \dots \dots \dots \dots 4.3$$

$$P_x = \frac{1}{N} (\frac{N_X}{N_A} P_A + \frac{N_X}{N_B} P_B + \frac{N_X}{N_C} P_C \dots \dots + \frac{N_X}{N_N} \dots \dots \dots \dots 4.4$$

Where P_X is a precipitation for the station of missed record, N is number of stations used in the computation, P_A, P_B, P_C….P_N are the respective precipitation at the index stations and N_A, N_B, N_C….N_N and N_X are the long term mean precipitation at the index stations and at station (x) under thought respectively.

3.3.1.2. Hydrological Data Analysis

Filling of Missing Stream Flow

The stream flow shows the strong serial relationship of the amount in one day is directly interrelated to the amount in the preceding and succeeding days particularly for periods of low flow or recession. In Genale river the high flow were happened on the rainy season which occurs in spring (March to May) and autumn (September to November) and it has a satisfactory stream flow records by having a small number of missing data for the period of (1988-2015). The mean monthly and annual stream flow data of Chenemesa gauging station is presented in Appendix: 1.

Sediment Rating Curve preparation

The measured sediment data of the Genale River was collected from MoWIE at Chenemesa gauging station which was not in continuous time step. Hence, to have full input data for the model it can be solved by using stream flow and measured suspended sediment data we can generate sediment load data in continuous time step, by means of developing sediment rating curve. The observed sediment concentration data was shown in Appendix: 2, which was used for sediment rating curve preparation. This sediment rating curve is broadly applied to estimate the sediment loads which are actually transported by the river. Generally, a sediment rating curve is plotted for presenting mean sediment concentration load as a function of discharge averaged in daily, monthly or any other time periods. Therefore using this curve the recorded discharges was converted into records of sediment concentration load and the overall correlation shall be obtained by:

$$S = a * Q^b \quad \ldots\ldots\ldots\ldots\ldots\ldots\ldots\ldots\ldots\ldots 4.6$$

Where, S is the sediment load in (ton/day), Q is daily stream flow in m^3/s, a and b are the regression constants.

Therefore since the observed values which are taken from the MoWIE were sediment concentration; so that the first work was to transform this flow discharges into sediment concentration load by using:

$$S = 0.0864 * Q * C \quad \ldots \ldots \ldots \quad 4.7$$

Where, S is sediment load which defined by (ton/day), Q stream flow given by (m^3/s), C is sediment concentration in (mg/l) and 0.0864 is conversion factor.

After the computation of sediment load concentration the establishment of the correlation among the continuous (daily time step) observed daily flow in cumec and the observed sediment concentration load (ton per day) was followed. Then from this relation the flow and sediment load has R^2 of 0.89% as shown in Figure (4.3).

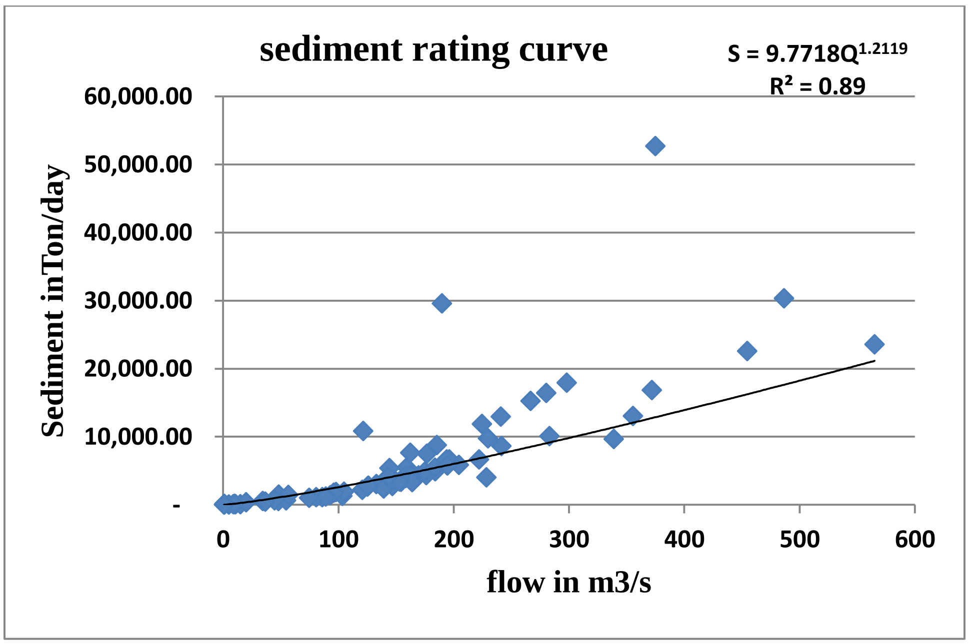

Figure 3.2 Sediment rating curve

$$\boldsymbol{S = 9.771Q^{1.2119}} \quad \ldots \ldots \ldots \quad \mathbf{4.8}$$

Where: - S = Suspended sediment mass transport rate (ton/day) and Q = discharge (m^3/s)

Depending on this equation and the historical flows observed at the gauging station near to Chenemesa monthly suspended sediment load were estimated and used for calibration and validation.

3.3.1.3. Spatial data analysis

Land use/cover change analysis

From the most important factors that affect the hydrological properties of the study area is the land use land cover. Therefore, to find the hydrological response units of the study area, LULC was considered as the main input data for SWAT model. The study was performed using Landsat image to describe the changes that comes due to LULC distribution in Genale sub basin in 24 years period from 1994 to 2017. Landsat TM, ETM+, EM+ were chosen for the period of 1994, 2000 and 2017 respectively. To minimize the seasonal deviation of plants distribution condition all the way through the year, the choosing of dates of the necessary data were made as far as possible in the same annual season of the required years.

A. image processing

The satellite images used in this study area were ortho-rectified for the Universal Transverse Mercator projection using datum WGS (World Geodetic System) 84 zone 37N. The image of 2000 was obtained from Ethiopian mapping agencies and the other two image data files were from (USGS) website and then extracted to (Tiff) file formats. The way or the method of the selection of the image for the specific area was depending on required date, sensor, path/row, resolution. Generally the producers and information about satellite image applied for this research were briefed in the following table.

Table 3.2-2 Satellite image information

Sensor	Scene no.	pass	Row	Acquisition date	Resolution(m)
TM	1	166	56	01/29/1994	30x30
TM	2	166	57	01/29/1994	30x30
TM	3	167	55	01/20/1994	30x30
TM	4	167	56	01/20/1994	30x30
TM	5	167	57	01/20/1994	30x30
TM	6	168	55	01/27/1994	30x30
TM	7	168	56	01/27/1994	30x30
ETM+	1	166	56	01/24/2000	30x30
ETM+	2	166	57	01/24/2000	30x30
ETM+	3	167	55	01/28/2000	30x30
ETM+	4	167	56	01/28/2000	30x30
ETM+	5	167	57	01/28/2000	30x30
ETM+	6	168	55	02/05/2000	30x30
ETM+	7	168	56	02/05/2000	30x30
ETM+	1	166	56	01/28/2017	30x30
ETM+	2	166	57	01/28/2017	30x30
ETM+	3	167	55	01/19/2017	30x30
ETM+	4	167	56	01/19/2017	30x30
ETM+	5	167	57	01/19/2017	30x30
ETM+	6	168	55	01/26/2017	30x30
ETM+	7	168	56	01/26/2017	30x30

Then using ERDAS imagine 2014 layer stacking image and mosaic of different scenes of images had been done.

Layer stacking images- it is the process that used to analyze and stacked the remotely sensed images that has different band to have a single multispectral. This allows different combinations of RGB to be shown in the view. Layer stacking is also commonly used to combine image derivatives with spectral bands for further analysis (i.e., layer stack an NDVI (normalized difference vegetation index) image with spectral bands for input to an image classification) (ERDAS imagine user manual, 2014).

Mosaic pro was used to combine different scene of images together so one large, cohesive image of an area can be created. Because of the different features of Mosaic Pro, we smooth these images before mosaicking them together as well as color balance them, or adjust the histograms of each image in order to present a better large picture(ERDAS imagine user manual, 2014).

After mosaicking of all images together then the larger image is cropped with respect to the size of study area. Sub setting is the process of clipping out of certain portion of an image for further processing. Sub setting of Genale sub-basin satellite image was performed using the layer stacked and mosaicked images by the shape file to make ready for classification.

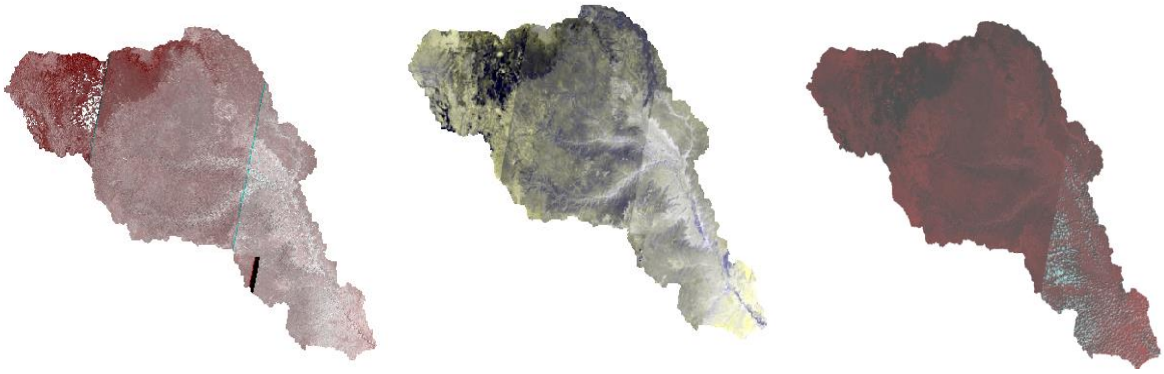

A, image of 1994 B, image of 2000 C, image of 2017

Figure 3.2 Satellite image of the study area after layer stack and mosaic

B. land use/cover image classification

The process of Image classification was transforming of the pixels of continuous raster image to the pre-determined LULC classes. In remote sensing, there are several image classification techniques. Their correctness is depend on the objective of land cover maps producer designed for and the analyst's awareness of an algorithms is using. However, in most cases different researchers are categorized the way of classification into three major groups: i.e. Supervised, unsupervised and hybrid.

For this specific study the classification was done by using ERDAS Imagine 2014, and unsupervised digital image classification technique was applied. It was done by connecting ERDAS EMAGINE 2014 software with Google earth pro to cross check the ground information about the types of land use land cover classes. To visualize the real ground information and to know different land use land cover categories, site visiting and Ganale Dawa master plan report was used as initial references. Hence, six categories of land use land cover were identified. This includes forest, woody land, cultivated land, grassland, bushland and bare land as described in Table below.

Table 3.2-3 Description of LULC used for change study from 1994 to 2017

Land use land cover change types	Descriptions
Forest	Areas dominated by natural high forests, which are large trees like coniferous and man-made trees
Woody land	This cover category was mapped mainly in areas falling next to forest, on hills and along river side and mixed with small bush land
Cultivated land	Includes state farms, mechanized private farms and small holder farms.
Bush land	Areas covered with mainly bush, shrubs and other small sized plant species (less than 3m)
Grass land	All areas covered with natural grass and small shrubs dominated by grass
Bare land	Areas of exposed surface

In general the classification of satellite image process was summarized in the following chart.

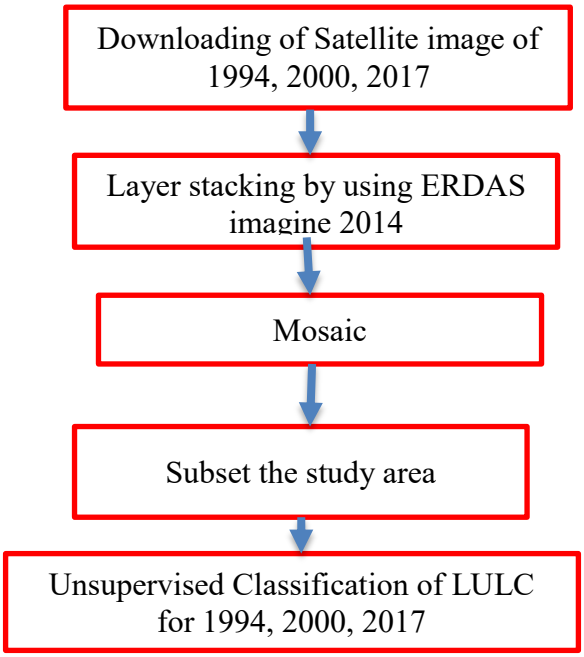

Figure 3.2 procedural steps of image classification

Soil data and analysis

Soil data of Genale Dawa basin were collected from MWIE. According to FAO the identified soil group is presented in appendix 3. Different soil may have different physical and chemical properties such as soil erodibility factor, hydraulic conductivity, infiltration capacity, organic carbon content etc. which influences the water balance and sediment yield from the sub-basin. For this case SWAT model requires the input soil physical and chemical properties for instance hydraulic conductivity, available water content, soil texture, bulk density and organic carbon content for each layers of soil profile.

The soil map is integrated with SWAT model through a user soil database that comprises the properties of soil which are arranged for every soil layers and imported to the SWAT user soil databases.

Digital elevation model (DEM)

The (DEM) is digital image of the geographic surface or elevation of every point at specific spatial resolution of the given area. (DEM) data was needed to analysis the flow accumulation, watershed delineation, stream networks and the quantitative description of geomorphologic characteristics of the catchments such as slope, aspect, altitude, etc., which is used for runoff estimation in SWAT model. A 20mby 20m resolution DEM of Ganale Dawa basin was download from the USGS. (Figure 4.5) and this DEM was used in SWAT model for watershed delineation and for further analysis.

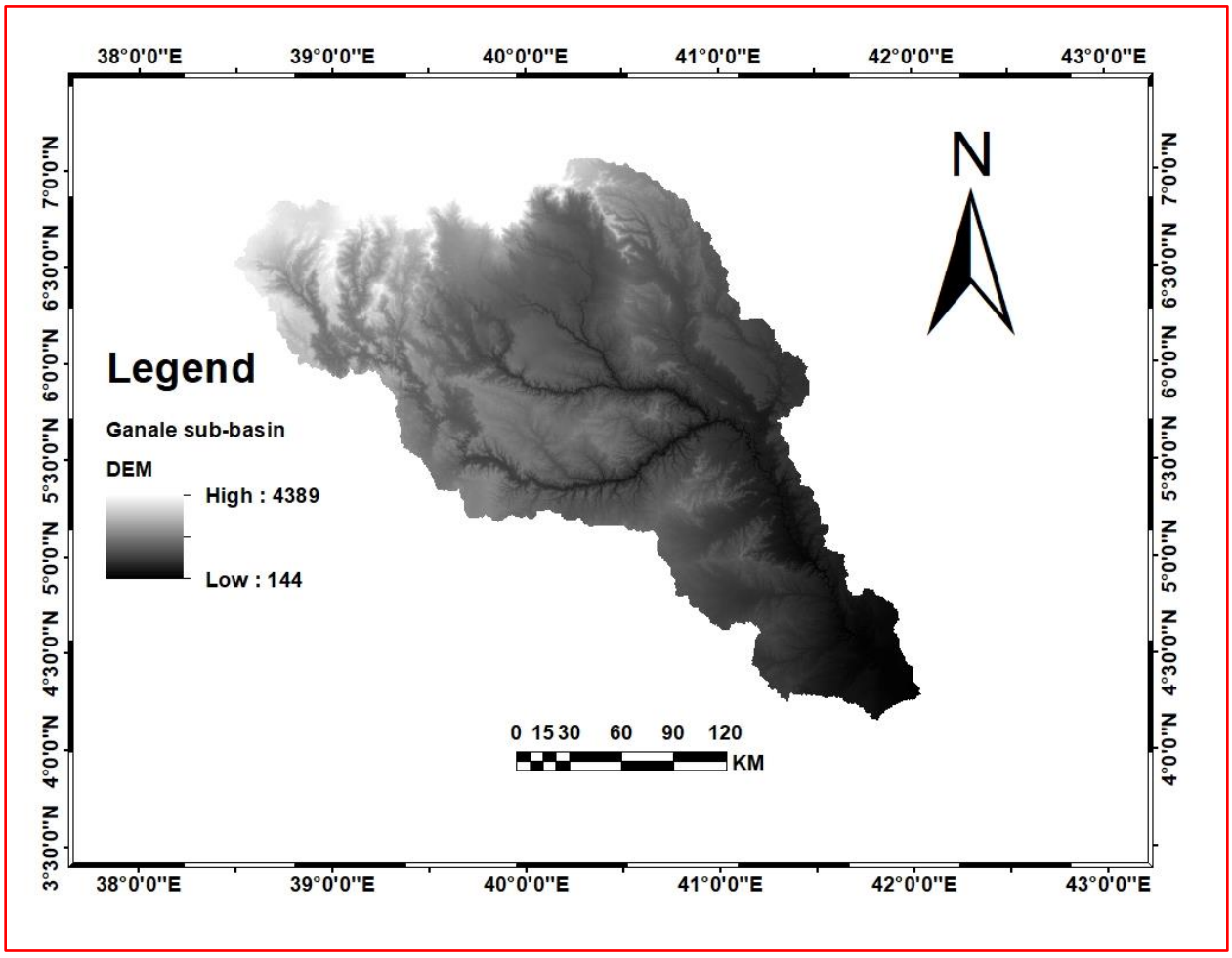

Figure 3.8 DEM of Ganale sub-basin

3.4. Model setup and input data processing

3.4.1. Watershed delineation

The first step of watershed delineation is started by SWAT project setup and followed by automatic water watershed delineation. Then the SWAT model helps the user for delineating watersheds and sub-basins using Digital Elevation Model (DEM). The size of DEM used for this study area was 20m by 20m grid cell resolution. The next step of this watershed delineation is stream definition based on DEM by the SWAT model using the flow patterns. The threshold area is estimated to define the origin of streams to have the small drainage area needed to form the origin of a stream. For this study the threshold area was taken 1147.41ha. Then after by adding watershed outlet manually, the outlet definition, the inlet definition, watershed outlet choosing and definition and lastly the calculation of the sub-basins parameters were done.

3.4.2. Hydrologic response units (HRU) definition analysis

Arc-SWAT was used to up load land use land cover, soil, and slope map with the integration of Arc GIS. Hence for these cases the delineated watershed was checked that the prepared LULC, slope and data of soil layers were overlapped 100%. The analysis of HRU consists of the classification of HRUs by slope classes in addition to land use and soils. In this case the sub-basin were divided into a number of hydrologic response units or HRUs) having unique soil and land use properties. Then after loading all LULC, soil and slope the map was reclassified to relate with the parameter found in the SWAT database.

According to the SWAT user's manual suggestion 10% threshold value for LULC, 10% for the soil and 20% for the slope were used to for this study area. Hence, Ganale sub-basin was divided into 2632 HRUs for land use land cover 1994 model, 2689 HRUs for land use 2000 model and 2449 HRUs for land use 2017model. Each HRU has a unique land use land cover, slope and soil combinations.

3.4.3. Weather data

The swat model requires weather data such as daily temperature, rainfall, relative humidity, wind speed, and sunshine from measured data. Then appealing this weather data to SWAT Weather Database program which was downloaded from internet to calculate SWAT WGEN Statistics such as the monthly daily average, standard deviation, probability of wet and dry days, skew coefficient dew point, and average number of precipitation days in the month from the stations.

3.5. Model Simulation

Modeling is defined as the process of organizing, synthesizing, and integrating component parts into a realistic representation of the prototype. The Models help sharpen the definition of hypotheses, define and categorize the state of knowledge, provide an analytical mechanism for studying the system of interest, and can be used to simulate experiments instead of conducting the experiments on the watershed itself.

For a better understanding of a hydrological condition in the detail analysis of the integrated water resources management the hydrological modeling is best method. Based on the procedure of explanation, hydrological models shall be categorized in to three main types(Cunderlik 2003)

1) Lumped models: in this case the parameter does not vary spatially among the sub-basins and as a result, sub-basin responses were estimated merely at the outlet of the sub-basin i.e. it do not for of each sub-basin. Usually in lumped model the parameters would not represent fully the physical features of the hydrologic processes and it contains some empiricism. The impact evaluation of spatial variability of the model parameters is done by using certain procedures for estimating effective values for the entire basin. The best commonly applied technique for this case was an area-weighted average. The lumped models were not usually applicable for the event-scale processes. If the primarily attention were for the discharge prediction only, then these models can provide as the good simulations results (Seifu 2015).

2) Semi-distributed models: Parameters of this model types are, partially allowable to vary in space by separating the basin into several smaller sub basins. There are two main types of semi-distributed models:

i) Kinematic wave theory models (KW models, like HEC-HMS), and

ii) Probability distributed models (PD models, like TOPMODEL).

The surface and subsurface flow equations of the physically based hydrological models are the simplified versions. In the PD models spatial resolution is considered for using the probability distributions of input parameters across the sub-basin. SWAT, HEC-HMS, HBV, are considered as semi-distributed models (Seifu 2015).

3) Distributed models: in this case the models are fully allowed to vary in space at the Resolution selected by the user. This kind of modeling type helps to integrate data relating to the spatial distribution of different parameter which varies in space and time to assess the impact of the spatial distribution on simulated result. These types of modeling system normally needs large amounts of data (may be inaccessible) to parameterize in every grid cell. But, if the main physical processes are applied or modeled in detail, it may give as the highest degree of accuracy (Seifu 2015).

3.5.1. Hydrologic Model Selection Criteria

There are different criteria that may be depend on the project types, because every project has its own particular requirements and needs. And also some criteria may be user dependent, like a personal interest for graphical user interface, computer operation system, input/output management and structure, or users add on expansibility. One of the main four selection criteria of the project-dependent, are (Cunderlik 2003)

- Required model outputs is important for the needed purpose to be estimated by the model – such as peak flow, event volume and hydrograph, long term flows
- Capability of the model to simulate the regulated reservoir for operation purpose and to estimate the single or continuous event was considered.
- Accessibility of input data – based on time and cost wise the model input data should be available easily.
- Price – usefulness of the project is also ?

In addition to the above criteria, adaptability of the hydrologic model, the type of the problem what I am addressing are also considered.

One of the various and mostly used conceptual models for assessment of surface water potential is SWAT model. SWAT model is the widely used in all over the world and in many parts of Ethiopia.

Therefore, SWAT model is selected for modeling the surface water potential in my study area based on the above criteria (Ibrahim 2018).

3.5.2. Reasons for selecting SWAT model

- The comparative impact of optional input data like variation in monitoring practices, climate, and vegetation/land use on soil erosion or sediment yield, runoff, or alternative variable of important would be calculated.
- To apply for large basin area and by low cost SWAT model is computationally efficient
- The model allows the users to consider long-term impacts.
- to support various watershed and water quality modeling studies the SWAT model can be applied.
- SWAT explicitly incorporates elevation/orographic impacts on precipitation and temperature.
- The SWAT model is designed to analysis the long term effects by using different flow data, meteorological data, and geographical data which is physical based model. (Seifu 2015).

3.5.3. Hydrologic modeling

The simulation of hydrologic process in watershed was done by SWAT model by dividing the watershed into sub watersheds depending on the drainage areas of a tributaries river. Sub-watershed also again more differentiated into HRU, based on the digital elevation model (DEM), land use land cover, weather data, slope and soil features.

The simulation of hydrologic watershed was done by two separate parts: the land phase and the routing phase. During land phase simulation the SWAT uses the following Water balance equation 4.9.

$$SW_t = SW_o + \sum_{i=1}^{t}\left(R_{day} - Q_{surf} - E_a - w_{seep} - Q_{gw}\right) \quad \text{4.9}$$

Where SW_t is the final soil water content given by (mm), SW_o is the initial soil water content on day I in (mm), t is the time in (days), R_{day} is the amount of precipitation on day I in (mm), Q_{surf} is the amount of surface runoff on day i given by (mm), E_a is the amount of evapo-transpiration on day i in (mm), W_{seep} is the amount of water entering the vadose zone from the soil profile on day i in (mm), and Q_{gw} is the amount of return flow on day i in (mm). From the above water balance equation SCS curve number method was applied depending on the obtainability of data.

$$Q_{surf} = \frac{(R_{day} - I_a)2}{(R_{day} - I_a + S)} \ldots \ldots \ldots \ldots \ldots \ldots 4.10$$

$$S = 25.4 * \left(\frac{1000}{CN} - 10\right) \ldots \ldots \ldots \ldots \ldots \ldots 4.11$$

Where S is the retention parameters, CN is curve number and R_{day} is the amount of precipitation on day i given by (mm)

In case of routing phase there are two options for routing the flow within the channel which was variable storage and Muskingum methods. The Muskingum routing method models the storage volume in a channel and/or reservoir length as a combination of wedge and prims storages whereas the variable storage uses simple continuity equation in the storage volume.

Therefore for this study the amount of stream flow that comes from the watershed were routed by variable storage and estimate or simulated by using Arc-SWAT model.

$$\Delta V = V_{in} - V_{out} = \Delta t \left(\frac{q_{in,1} + q_{in,2}}{2}\right) + \Delta t \left(\frac{q_{out,1} + q_{out,2}}{2}\right) \ldots \ldots \ldots \ldots 4.12$$

Where, Δt was the length of the time step in (s), $q_{in,1}$ is the inflow rate at the beginning of the time step in (m^3/s), $q_{in,2}$ was the inflow rate at the end of the time step given by(m^3/s), $q_{out,1}$ was the outflow rate at the beginning of the time step (m^3/s), $q_{out,2}$ was the outflow rate at the end of the time step (m^3/s), V_{out} was the storage volume at the starting of the time step given by (m^3) and V_{in} was the storage volume at the end of the time step given by (m^3).

3.5.4. Sediment modeling

The SWAT uses the modified Universal Soil Loss Equation (MUSLE) to estimate the erosion and sediment yield.

$$Sed = 118 * (Q_{Surf} * q_{peak} * A_{hru})^{0.56} * K_{USLE} * C_{USLE} * P_{USLE} * LS_{USLE} * CFRG \ldots \ldots \ldots 4.13$$

Where Sed is the sediment yield on a given day measured in metric tons, Qsurf is the surface runoff from the watershed given by mm/ha, q_{peak} is the peak runoff rate measured in cubic meter per second, A_{hru} is the area of HRU, K_{USLE} is the USLE soil erodability factor, C_{USLE} is the USLE land cover and management factor, P_{USLE} is the USLE support practice factor, LS_{USLE} is the USLE topographic factor, and CFRG is the coarse fragment factor.

Similar to the flow the estimated sediment yield was routed during simulation. In watershed delineation at least one main routing reach was calculated and the routed results at each outlet of the sub-basin were found. Hence, the sediment derived from upper part of sub-basin is routed through these reaches to be added to downstream reaches.

3.6. Sensitivity analysis

While the number of parameters in a model is large due to a large number of processes considered or for the reason that of the model structure itself, the calibration and validation processes becomes complex. In such cases, sensitivity analysis was useful to find and rank parameters that have considerable impact on particular models outputs of interest. There are two types of sensitivity analysis (Global sensitivity and one at a time sensitivity analysis).

Global sensitivity analysis: - it was computed by multiple regression system that regresses the calculated result beside the objective function of the values. In this type of sensitivity analysis A t-stat was the method applied to find the importance of each parameter comparatively. T-stat was given by the coefficient of parameter divided by its standard error and it is a measure of the accuracy with which the regression coefficient is measured. Therefore, if a coefficient is large (absolute value) relative to its standard error, then it is probably different from 0 and the parameter is more sensitive. On the other way, p-value shows the importance of the sensitivity and hereafter a value near to zero has more importance. Therefore ranking in both conditions i.e. (t-stat and p-value) shall give similar results i.e. the parameter will have the same rank either it is ranked based on the t-stat or p-value (Abbaspour 2014).

One-at-a-time sensitivity analysis: - indicates the sensitivity of one variable at a time when the other parameters are constant.

Therefore, based on the global sensitivity analysis method and by reviewing previously calibrated in the Ganale Dawa basin more sensitive parameters were selected for calibration and validation process.

3.7. Model Performance Evaluation

In order to evaluate the performance of SWAT model to decide the quality and reliability of the predicted result it is mandatory to compare with the observed values by following methods. For goodness-of-fit measures the model estimation would be applied for the period of the calibration and validation. These are explained numerically to show the model performance by using the coefficient of determination (R^2) and Nash-Sutcliffe simulation efficiency (NSE)(Nash 1970).

The regression coefficient (R^2) is the square of the Pearson product–moment correlation coefficient and defines the quantity of the general differences in the measured data that shall described by the model. As R^2 close to 1, the agreement between the simulated and the measured flows and sediment load is the higher and it will be calculated by,

$$R^2 = \frac{(\sum[Qsi - Qsi_{av}]\,[Qob - Qob_{av}])^2}{\sum[Qsi - Qsi_{av}]^2 \sum[Qob - Qob_{av}]^2} \quad \ldots\ldots\ldots\ldots\ldots\ldots\ldots\ldots\ldots\ldots\ldots\ldots\ldots\ldots\ldots\ldots\ldots\ldots\ldots\ldots\ldots\ldots 3.17$$

Where, Qob is measured value, Qob_{av} is the average measured value. Qsi predicted value, Qsi_{av} average predicted value.

NSE was also shows the degree of appropriateness of measured and the simulated data and it is obtained by the following equation.

$$NSE = 1 - \frac{\sum(Qob - Qsi)^2}{\sum(Qob - Qob_{av})^2} \quad \ldots\ldots\ldots\ldots\ldots\ldots\ldots\ldots\ldots\ldots\ldots\ldots\ldots\ldots\ldots\ldots\ldots\ldots\ldots\ldots\ldots\ldots\ldots 3.18$$

Where, Qob is measured value, Qob_{av} is the average measured value. Qsi predicted value. The value of NSE ranges from 1 (best) to negative infinity. The efficiency of NSE express how much the plot of measured against simulated result much the 1:1 line. If the measured data is the similar with all simulations result, NSE is 1. If the NSE is found between 0 and 1, there are the vaiation between observed and simulated results. (Nash 1970).

The capability of the model to appropriately calculate the basic stream flow and sediment yield shall be assessed through by sensitivity analysis i.e. model calibration and model validation (White and Chaubey 2005).

3.8. Model calibration and validation

3.8.1. Model calibration

Model calibration was done by adjusting model sensitive parameters to match the simulated result with the observed data as much as possible within the accepted range of deviation. To reduce the uncertainty of results the previous thesis done in the basin was reviewed and swat cup 2012 program was used. In this study two step of calibration process was done: for flow and sediment calibration. First stream flow calibration was done based on monthly time step at the outlet of sub-basin 162 at Chenemesa station and then for sediment.

Chenemesa station was preferred because of the availability of observed flow and sediment data and located near to reservoir. Based on the available model input data the time period used for calibration modeling was 1988-2005 including model warm up period of two years.

3.8.2. Model validation

Model validation is testing of the calibrated model results with independent data set without any adjustment. The validation of flow and sediment was executed at similar station with the calibration and the statistical criteria (R2, NSE) was applied to make it within the accepted limits (R2>0.6, NSE>0.5). Thus, a performance evaluation criterion was calculated using by Equation 4.14, 4.15. Based on the available model input data the time period used for validation modeling was 2006-2015.

$$R^2 = \frac{(\sum[Qsi - Qsi_{av}]\,[Qob - Qob_{av}])^2}{\sum[Qsi - Qsi_{av}]^2 \sum[Qob - Qob_{av}]^2} \quad \ldots\ldots 4.14$$

$$NSE = 1 - \frac{\sum(Qob - Qsi)^2}{\sum(Qob - Qob_{av})^2} \quad \ldots\ldots 4.15$$

3.9. Analysis of land use land cover change of the study area

This study was able to analysis the influence of three different years land use land cover dynamics on Genale Dawa dam three sedimentation. So the three land use were prepared from the satellite image and classified by unsupervised classification technique using ERDAS imagine software. Using the newly classified land use land cover map i.e. 1994, 2000, and 2017, and keeping daily climate and other input data as a constant, SWAT simulation, calibration and

validation was done for each model with respected period. After calibration and validation of each model to show the variability of runoff and sediment load from the three models (land use 1994, land use 2000, land use 2017), then the simulated stream flow and sediment result of each year were compared.

CHAPTER FOUR

4. RESULT AND DISCUSSION

4.1. Land use land cover classification

The study area's LULC was classified into six (forest land, woody land, cultivation land, bush land, grass land, and bare land) classes for the three base periods to get the spatial distribution of land use land cover which were used in the swat modeling. The classification was done depending on master plan of Ganale Dawa basin report and site visiting of some parts of the study area for the visualization of actual site.

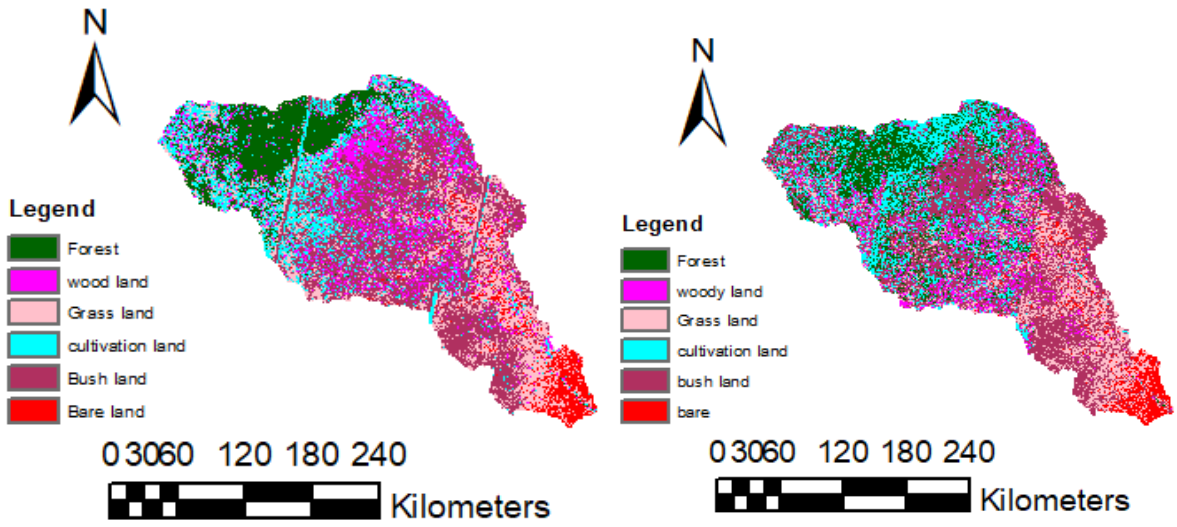

A) LULC map of Ganale sub-basin in1994 **B)** LULC map of Ganale sub-basin in 2000

Figure 4.1 Land use land cover map of Genale sub-basin in 1994 and 2000

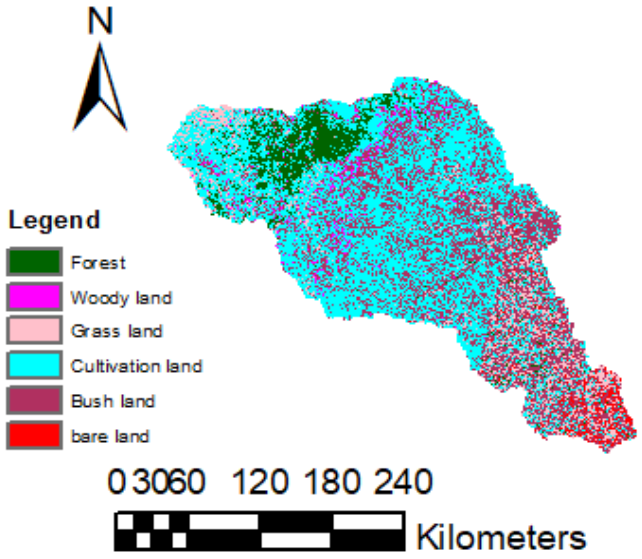

Figure 4.2 Land use land cover map of Ganale sub-basin in 2017

4.2. Analysis of land use land cover changes

As it is shown in table 5.1, and figure 5.2 in 1994, 15.30% of the Ganale sub-basin was covered by forest land, 12.46% of woody land, and 12.44% by cultivation land 19.48 % by grass land, 35.63% was bush land and 4.7% was bare land. In this year the bush land was the most dominant land use land cover type in the study area covering of 1,986,421.40ha (35.63%,) followed by grass land 1,085,878.74 ha (19.48 %) and bare land were the least dominant classes.

In the case of 2000 year of land use land cover bush land use type was the dominant by covering an area of 2,319,767.08ha (41.61%), followed by cultivation land covering of 1,005,973.84 ha (18.04%), 902,716.31ha (16.19%), forest 735,259.66 ha (13.19 %), woody land 417,180.82 (7.48%) and bare land 194,518.7 (3.49%).

And also for the case of 2017 year of land use land cover modeling cultivation land use type was the most dominant by covering an area of 2,949,856.46ha (52.91%), followed by bush land 1662959.8ha (29.83%), grass land, forest land, and bare land were least dominant.

Table 4-1 LULC change of Ganale sub-basin during the period of 1994, 2000 and 2017.

LULC types	1994		2000		2017		change from 1994 to 2017	
	Ha	%	Ha	%	Ha	%	ha	%
forest	852984.2	15.3	735259.7	13.2	387772.2	6.96	-465212	-8.34
woody land	694537.7	12.46	417180.8	7.5	18956.0	0.34	-675582	-12.1
cultivation land	693805.1	12.44	1005974	18	2949857	52.91	2256051	40.5
bush land	1986421	35.63	2319767	41.6	1662959.8	29.8	963435.1	-5.80
grass land	1085879	19.5	902716.3	16.2	477308.2	8.6	-608570	-10.9
bare land	261789.2	4.7	194518.7	3.5	78563.8	1.4	-183226	-3.3

According to Ganale Dawa master plan report, the studies conducted in 1984 and 2004 the most dominant land cover was bush land and most of land cover was converted to cultivated land, which was similar with this study even if the report were done based on the basin level. In 2004 the cultivated land, forest, woodland, bushland, grass land and bare land was 15.65%, 5.07%, 5%, 16.3%, 50%, 6.25%. In general during the three modeling period the considerable cultivated land has been increased and other land use were decreased. This may be because of population growth that caused the increase of cultivation and deforestation of forest land and woody land for other purposes.

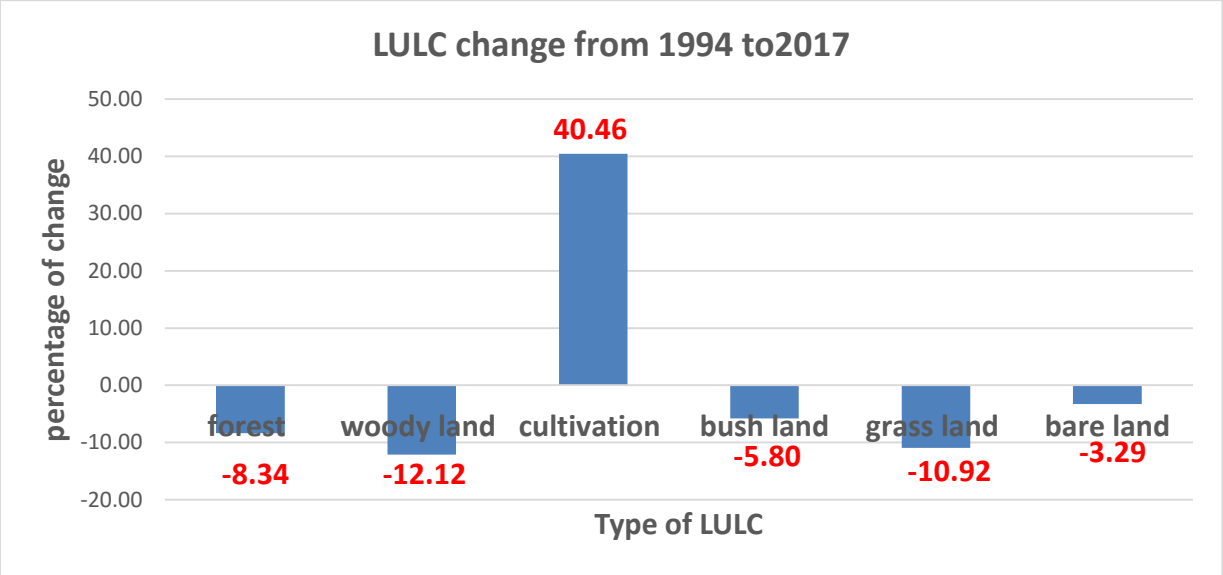

Figure 4.3 Percentage of land use land cover from 1994 to 2017

4.3. Sensitivity analysis

Sensitivity analysis was done by using Swat-cup by global sensitivity method to identify which model parameters are more sensitive. Sensitivity analysis was carried out for the period of 18 (eighteen) years at 162 sub-basin number where the gauged data is found for flow and sediment calibration and validation. The parameter identification was done during calibration by using monthly flow data from 1990 to 2005 for land use 1994, 2000, and 2017 which include two year for model warm-up period and twelve years for model validation period from 2006-2015.

According to the result from global sensitivity analysis, Base flow alpha factor (ALPHA_BF), Effective hydraulic conductivity in tributary channel alluvium (CH_K1), Effective hydraulic conductivity in the main channel (CH_K2) and other as shown by rank order in the tables 5.2, 5.3, and 5.4 was the most sensitive parameters for the flow. Manning number (n) constants in channel (CH_N2), Initial SCS CN II value (CN2), USLE soil erodibility factor (USLE_K), Soil evaporation compensation (ESCO) and others shown in table 5.5, 5.6, 5.7 are the most sensitive parameters.

Now, t-stat provides as a degree of sensitivity and therefore the more in absolute values are the most sensitive. In addition P-value shows the importance of sensitivity which means when the value was near to zero it has more impact. As a result, giving a ranking in both way (t-stat or P value) shall is similar.

Table 4-2 Rank of flow parameter based on t-value and p-value for LULC of 1994

Parameters	Description of parameters	t-Stat	P-Value	Rank
2:V__ALPHA_BF.gw	Base flow alpha factor	5.96	0.00	1
19:V__CH_K1.sub	Effective hydraulic conductivity in tributary channel alluvium	-3.98	0.00	2
18:V__CH_K2.rte	Effective hydraulic conductivity in the main channel	-3.63	0.00	3
21:V__RCHRG_DP.gw	Deep aquifer percolation fraction	3.04	0.00	4
6:R__HRU_SLP.hru	Average slope steepness	2.41	0.02	5
8:R__SOL_AWC(..).sol	Available water capacity of the soil layer (mm/mm).	1.99	0.05	6
11:V__ESCO.hru	Soil evaporation compensation	-1.60	0.11	7
9:R__SOL_K(..).sol	Saturated hydraulic conductivity (mm/hr)	1.47	0.14	8
4:V__GWQMN.gw	threshold depth of water in the shallow aquifer for return flow to occur	-1.43	0.15	9
5:V__EPCO.bsn	Plant evaporation compensation factor unit-less	-1.42	0.16	10
14:R__SOL_Z(..).sol	Soil depth (for each layer)	-1.35	0.18	11
20:V__OV_N.hru	Manning's "n" value for Overland flow	1.31	0.19	12
12:V__CH_N2.rte	Manning's "n" value for the main channel	-1.28	0.20	13
17:V__SURLAG.bsn	Surface runoff lag coefficient	1.24	0.22	14
1:R__CN2.mgt	SCS runoff curve number	-0.56	0.58	15
13:R__SLSUBBSN.hru	Average slope length (m)	-0.55	0.58	16
3:V__GW_DELAY.gw	Groundwater revap coefficient	-0.53	0.59	17
7:V__CANMX.hru	Maximum Canopy Index (mm)	-0.47	0.64	18
15:V__REVAPMN.gw	Threshold depth of water in the shallow	-0.44	0.66	19
10:V__GW_REVAP.gw	Groundwater revap coefficient	-0.39	0.69	20
16:R__SOL_ALB(..).sol	Soil Albedo	0.17	0.87	21

Table 4-3 Rank of flow parameter based on p-value and t-value for LULC of 2000

Parameter Name	Description of parameters	t-Stat	P-Value	rank
8:V__SOL_AWC(..).sol	Available water capacity of the soil layer (mm/mm).	4.93	0.00	1
2:V__ALPHA_BF.gw	Base flow alpha factor	4.74	0.00	2
19:V__CH_K1.sub	Effective hydraulic conductivity in tributary channel alluvium	-3.39	0.00	3
18:V__CH_K2.rte	Effective hydraulic conductivity in the main channel	-3.18	0.00	4
4:V__GWQMN.gw	threshold depth of water in the shallow aquifer for return	2.74	0.01	5
11:V__ESCO.hru	Soil evaporation compensation	-2.45	0.02	6
10:V__GW_REVAP.gw	Groundwater revap coefficient	2.37	0.02	7
21:V__RCHRG_DP.gw	Deep aquifer percolation fraction	-1.89	0.06	8
7:V__CANMX.hru	Maximum Canopy Index (mm)	1.88	0.06	9
9:R__SOL_K(..).sol	Saturated hydraulic conductivity (mm/hr)	1.42	0.16	10
1:R__CN2.mgt	SCS runoff curve number	-1.38	0.17	11
5:V__EPCO.bsn	Plant uptake compensation factor	-1.31	0.19	12
6:R__HRU_SLP.hru	Average slope steepness	1.31	0.19	13
3:V__GW_DELAY.gw	Groundwater delay	-1.23	0.22	14
15:V__REVAPMN.gw	Threshold depth of water in the shallow	-1.23	0.22	15
16:R__SOL_ALB(..).sol	Soil Albedo	1.19	0.23	16
20:V__OV_N.hru	Manning's "n" value for Overland flow	1.04	0.30	17
12:V__CH_N2.rte	Manning coefficient for channel (unit less)	-0.69	0.49	18
17:V__SURLAG.bsn	Surface runoff lag coefficient	0.60	0.55	19
13:R__SLSUBBSN.hru	Average slope length (m)	0.33	0.74	20
14:R__SOL_Z (..).sol	Soil depth (for each layer)	-0.17	0.87	21

Table 4-4 Rank of flow parameter based on p-value and t-value for LULC of 2017

Parameter Name	Description of parameters	t-Stat	P-Value	rank
2:V__ALPHA_BF.gw	Base flow alpha factor	4.72	0.00	1
19:V__CH_K1.sub	Effective hydraulic conductivity in tributary channel alluvium	-3.75	0.00	2
18:V__CH_K2.rte	Effective hydraulic conductivity in the main channel	-2.96	0.00	3
8:R__SOL_AWC(..).sol	Available water capacity of the soil layer (mm/mm).	2.26	0.03	4
1:R__CN2.mgt	SCS runoff curve number	-2.18	0.03	5
20:V__OV_N.hru	Manning's "n" value for Overland flow	1.94	0.05	6
11:V__ESCO.hru	Soil evaporation compensation	-1.86	0.06	7
9:R__SOL_K(..).sol	Available water capacity of the soil layer (mm/mm).	1.76	0.08	8
21:V__RCHRG_DP.gw	Deep aquifer percolation fraction	1.63	0.10	9
6:R__HRU_SLP.hru		1.49	0.14	10
3:V__GW_DELAY.gw	Groundwater delay	-1.46	0.15	11
5:V__EPCO.bsn	Plant uptake compensation factor	-1.40	0.16	12
17:V__SURLAG.bsn	Surface runoff lag coefficient	1.31	0.19	13
14:R__SOL_Z(..).sol	Soil depth (for each layer)	-1.18	0.24	14
12:V__CH_N2.rte	Manning coefficient for channel (unit less)	-1.17	0.24	15
16:R__SOL_ALB(..).sol	Soil Albedo	0.46	0.65	16
7:V__CANMX.hru	Maximum Canopy Index (mm)	0.42	0.67	17
15:V__REVAPMN.gw	Threshold depth of water in the shallow	-0.41	0.68	18
10:V__GW_REVAP.gw	Groundwater revap coefficient	0.21	0.84	19
13:R__SLSUBBSN.hru	Average slope length (m)	-0.14	0.89	20
4:V__GWQMN.gw	threshold depth of water in the shallow aquifer for return	0.05	0.96	21

Table 4-5 Rank of Sediment parameter based on p-value and t-value for LULC of 1994

Parameter Name	Description of parameters	t-Stat	P-Value	rank
2:V__CH_N2.rte	Manning's "n" value for main channel	6.11	0.00	1
5:V__ESCO.hru	Plant uptake compensation factor	5.06	0.00	2
17:V__CH_COV2.rte	Channel Cover factor	-3.11	0.00	3
19:R__CN2.mgt	Initial SCS CN II value	3.00	0.00	4
6:V__ALPHA_BF.gw	Base flow Alpha Factor (days)	2.33	0.02	5
21:R__RSDCO.bsn	Residue decomposition coefficient	2.20	0.03	6
13:R__SOL_AWC(..).sol	Available water capacity of the soil layer (mm/mm)	-2.08	0.04	7
10:V__SPEXP.bsn	Exponential-factor-for-channel sediment routing	-1.66	0.10	8
3:V__EPCO.hru	Plant uptake compensation factor	1.56	0.12	9
8:V__CH_K2.rte	Effective hydraulic conductivity in main channel alluvium.	-1.48	0.14	10
20:R__FFCB.bsn	Initial soil water storage expressed as a fraction of field capacity water content	1.24	0.22	11
11:R__SLSUBBSN.hru	Average slope length (m)	1.24	0.22	12
4:R__SOL_Z(..).sol	Soil depth (mm)	-1.23	0.22	13
9:R__USLE_P.mgt	Support Practice Factor	-0.68	0.50	14
18:V__CANMX.hru	Maximum Canopy Index (mm)	-0.66	0.51	15
1:R__USLE_K(..).sol	USLE soil erodibility factor	0.53	0.60	16
16:V__CH_COV1.rte	Channel Erodibility factor	0.48	0.63	17
12:V__SURLAG.bsn	Surface runoff lag time [days]	-0.44	0.66	18
15:R__SOL_K(..).sol	Soil conductivity (mm/h)	-0.31	0.76	19
14:R__SLSOIL.hru	Slope length for lateral subsurface flow	-0.05	0.96	20
7:V__SPCON.bsn	Linear factor for channel sediment routing.	0.03	0.98	21

Table 4-6 Rank of sediment parameter based on p-value and t-value for LULC of 2000

Parameter Name	Description of parameters	t-Stat	P-Value	rank
19:R__CN2.mgt	Initial SCS CN II value	-16.6	0.00	1
4:R__SOL_Z(..).sol	Soil depth (mm)	3.70	0.00	2
2:V__CH_N2.rte	Manning's “n” value for main channel	2.78	0.01	3
5:V__ESCO.hru	Soil evaporation compensation	2.21	0.03	4
1:R__USLE_K(..).sol	USLE soil erodibility factor	-2.19	0.03	5
8:V__CH_K2.rte	Effective Channel Hydraulic Conductivity (mm/h)	-2.12	0.04	6
13:R__SOL_AWC(..).sol	Available water capacity of the soil layer (mm/mm)	-1.76	0.08	7
3:V__EPCO.hru	Plant uptake compensation factor	1.67	0.10	8
6:V__ALPHA_BF.gw	Base flow Alpha Factor (days)	-1.66	0.10	9
18:V__CANMX.hru	Maximum Canopy Index (mm)	1.43	0.16	10
10:V__SPEXP.bsn	Exponential-factor-for-channel sediment routing	-1.12	0.27	11
9:R__USLE_P.mgt	Support Practice Factor	1.08	0.29	12
17:V__CH_COV2.rte	Channel Cover factor	0.81	0.42	13
16:V__CH_COV1.rte	Channel Erodibility factor	0.69	0.49	14
15:R__SOL_K(..).sol	Soil conductivity (mm/h)	0.66	0.51	15
7:V__SPCON.bsn	Linear factor for channel sediment routing.	-0.65	0.52	16
20:R__FFCB.bsn	Initial soil water storage expressed as a fraction of field capacity water content	0.64	0.52	17
11:R__SLSUBBSN.hru	Average slope length (m)	0.54	0.59	18
21:R__RSDCO.bsn	Residue decomposition coefficient.	-0.49	0.62	19
12:V__SURLAG.bsn	Surface runoff lag time [days]	-0.20	0.84	20
14:R__SLSOIL.hru	Slope length for lateral subsurface flow	0.16	0.88	21

Table 4-7 Rank of sediment parameter based on p-value and t-value for LULC of 2017

Parameter Name	Description of parameters	t-Stat	P-Value	Rank
1:R__CN2.mgt	Initial SCS CN II value	-14.60	0.00	1
19:R__USLE_K (..).sol	USLE soil erodibility factor	-3.40	0.00	2
16:R__SOL_K (..).sol	Soil conductivity (mm/h)	-2.36	0.02	3
9:R__SLSUBBSN.hru	Average slope length (m)	-2.28	0.03	4
10:V__SURLAG.bsn	Surface runoff lag time [days]	-1.90	0.06	5
7:V__SPEXP.bsn	Exponential-factor-for-channel sediment routing	-1.75	0.08	6
12:V__ESCO.hru	Soil evaporation compensation factor	1.55	0.12	7
3:V__SPCON.bsn	Linear factor for channel sediment routing	1.24	0.22	8
4:V__CH_N2.rte	Manning's“n”value for main channel	-1.24	0.22	9
8:V__CANMX.hru	Maximum Canopy Index (mm)	1.20	0.23	10
5:V__CH_K2.rte	Effective Channel Hydraulic Conductivity (mm/h)	-1.05	0.30	11
13:R__SOL_AWC(..).sol	Available water capacity of the soil layer (mm/mm)	0.93	0.35	12
18:V__CH_COV2.rte	Channel Cover factor	-0.66	0.51	13
2:V__ALPHA_BF.gw	Base flow Alpha Factor (days)	-0.66	0.51	14
15:R__SLSOIL.hru	Slope length for lateral subsurface flow	-0.64	0.52	15
17:V__CH_COV1.rte	Channel Erodibility factor	0.44	0.66	16
11:V__EPCO.hru	Plant uptake compensation factor	0.40	0.69	17
6:R__USLE_P.mgt	Support Practice Factor	0.31	0.76	18
14:R__SOL_Z(..).sol	Soil depth (mm)	0.12	0.91	19

4.4. Model calibration and validation

4.4.1. Flow calibration

After the sensitivity analysis has been identified, the calibration of SWAT model of simulated stream flow has been made using monthly observed flow data at an outlet of Chenemesa station or 162 sub-basin number outlets where gaging station was found. Once adjusting of the selected parameters as highly sensitive to flow as described under the sensitivity analysis section and using SWAT-CUP software SUFI 2 program for the three models i.e. for LULC 1994, LULC 2000, and LULC 2017 the result obtained were shown in table 5.8, 5.9, 5.10 and figure 5.5, 5.6, 5.7 below. Therefore the calibration was good or in acceptable ranges.

Table 4-8 Summary of flow calibration performance criteria result

performance criteria	1994	2000	2017
R^2	0.66	0.61	0.70
NS	0.63	0.58	0.65

The monthly simulated and observed flow at the outlet of the sub-basin number 162 were plotted for graphic judgment in Figure 5.4, 5.5 and 5.6 which are the graphical representation of calibration.

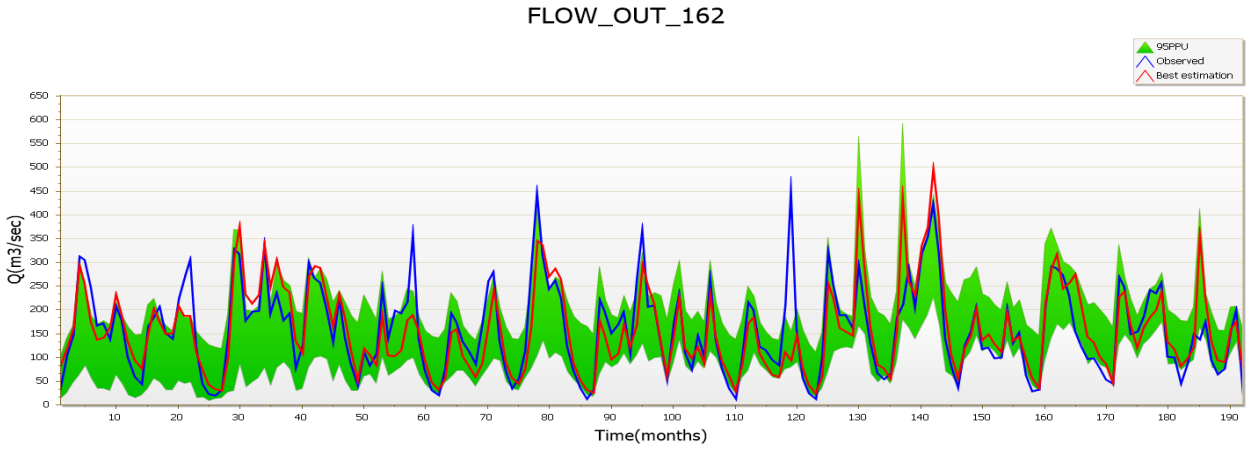

Figure 4.4 Comparison of the observed data with the simulated monthly flow for 1994 modeling.

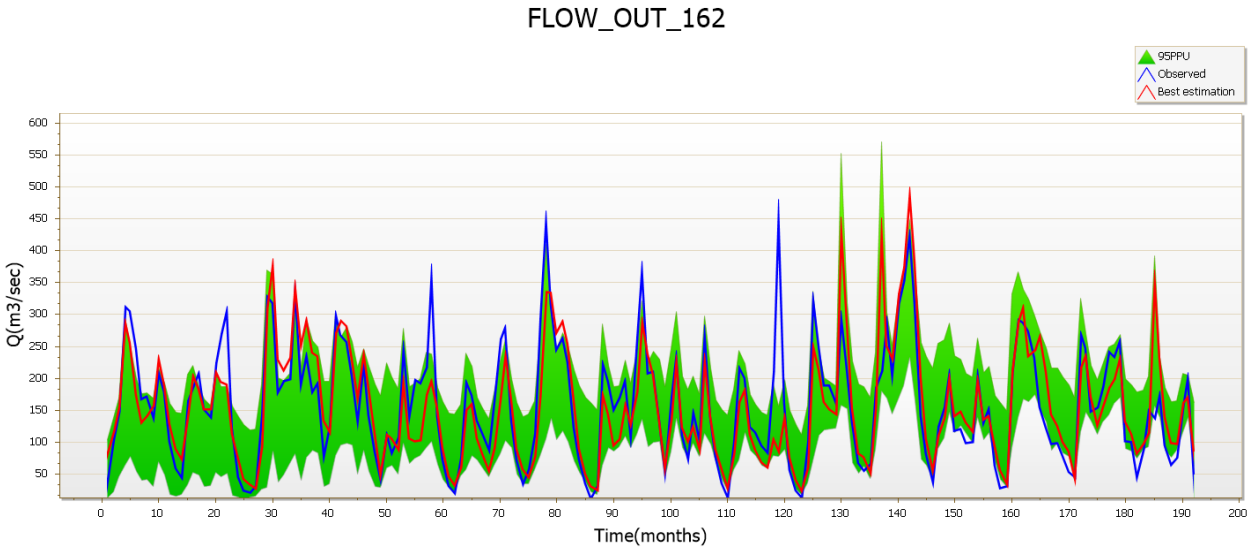

Figure 4.5 Comparison of the observed data with the simulated monthly flow for 2000 modeling.

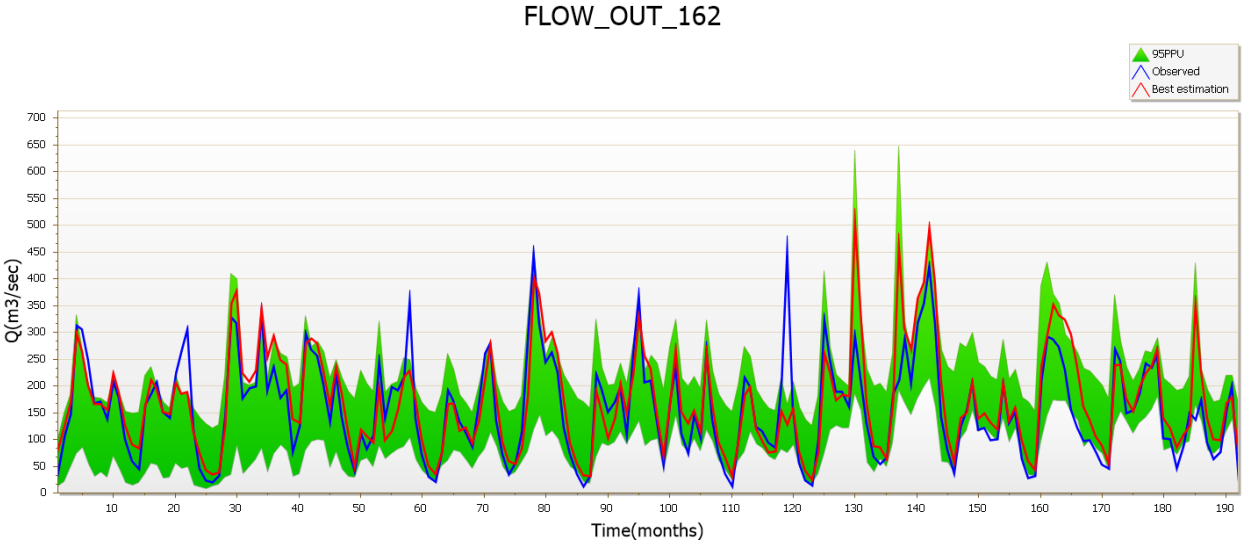

Figure 4.6 Comparison of the observed data with the simulated monthly flow for 2017 modeling.

4.4.2. Flow validation

Model validation was done with the observed flow data at similar location, however for the period of 2006 to 2015 without any adjustment of the calibrated parameters. As shown in the table 5.9, the result of coefficient of determination (R^2) and Nush Sutcliffe efficiency (NS) for LULC 1994 model were 0.69, 0.64 LULC 2000 were 0.69, 0.65 and LULC 2017 were 0.71, 0.66 respectively. Therefore, the outcome obtained was good or in acceptable ranges.

Table 4-9 Summary of flow validation performance criteria result

performance criteria	1994	2000	2017
R^2	0.69	0.69	0.71
NS	0.64	0.65	0.66

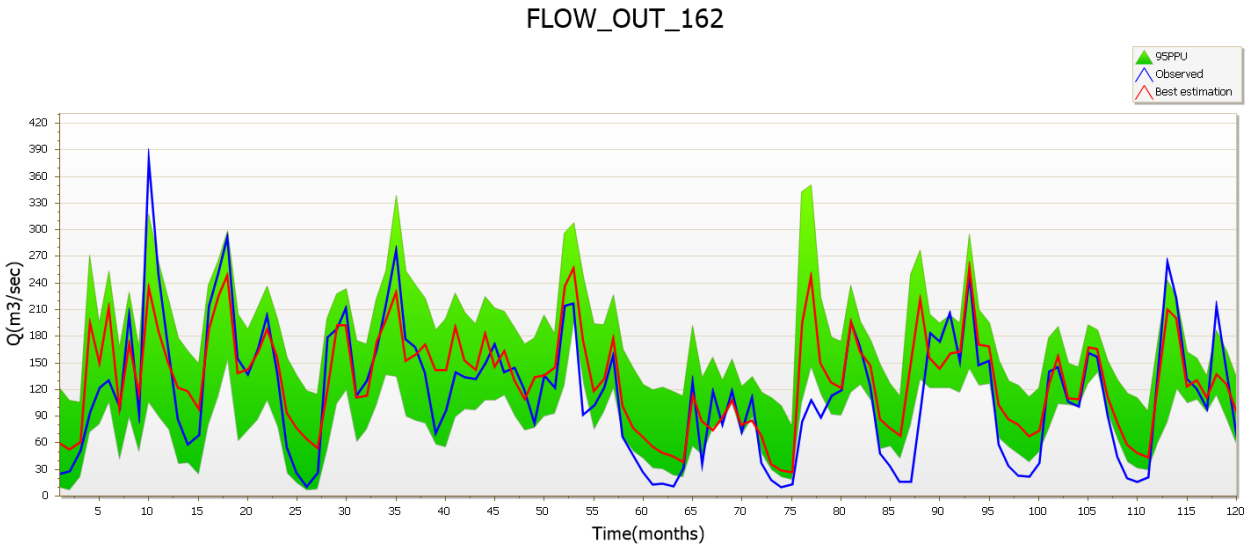

Figure 4.7 Comparison of the observed data with the simulated monthly flow for 1994 modeling.

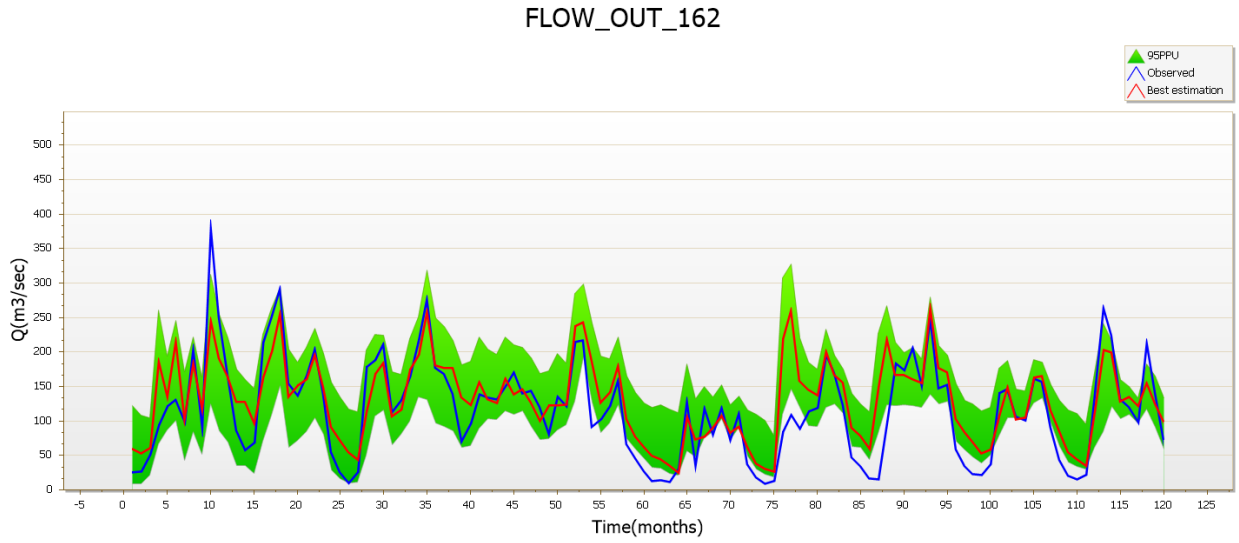

Figure 4.8 Comparison of the observed data with the simulated monthly flow for 2000 modeling.

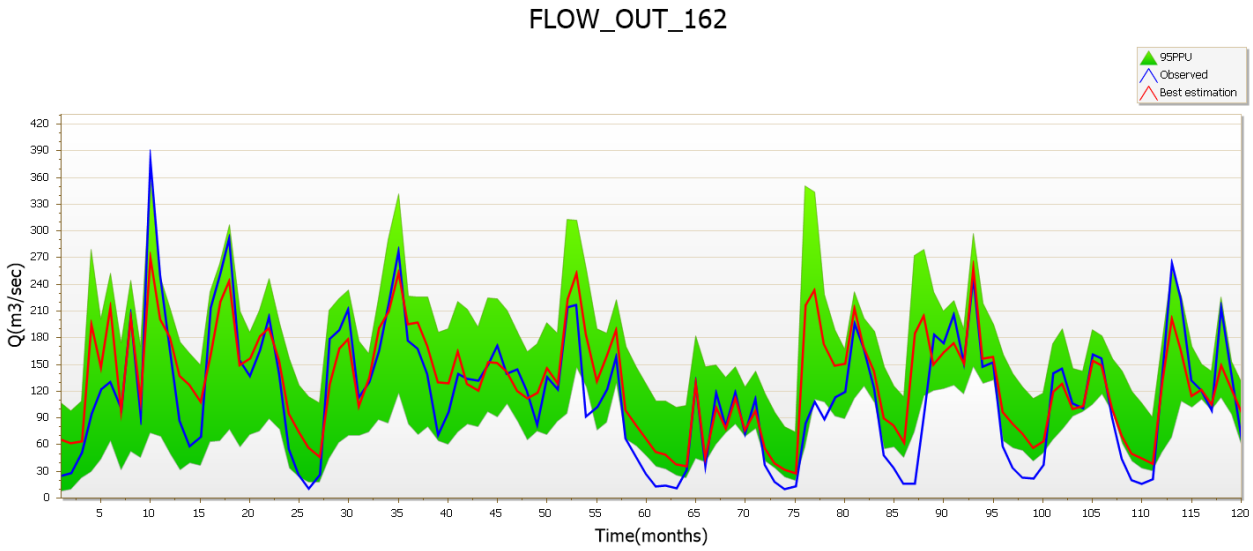

Figure 4.9 Comparison of the observed data with the simulated monthly flow for 2017 modeling.

4.4.3. Sediment calibration

The calibrations of sediment yield for Genale sub-basin was carried out depending on the selected sensitive parameters listed in sensitivity analysis section and have an impact on the predicted outcome when altered for sediment yield and by changing value of parameters by trial and error within the permissible limit. The calibration was done by SWAT-CUP software SUFI 2 program for the years 1988 to 2005 for all land use land cover. The model performance evaluation calculated from the predicted and measured monthly sediment loads to the calibration time was, coefficient of determination (R^2) and Nash-Sutcliffe model efficiency (NSE) as shown on table 5.10.

Table 4-10 Summary of sediment calibration performance criteria result

performance criteria	1994	2000	2017
R^2	0.63	0.68	0.67
NS	0.57	0.64	0.51

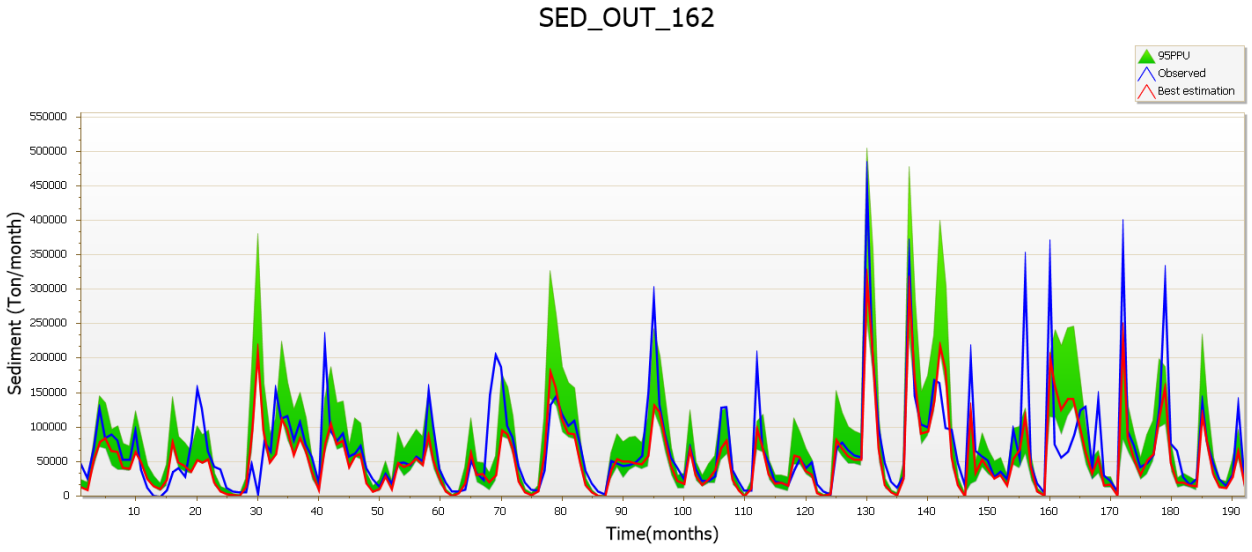

Figure 4.10 Comparison of the observed data with the simulated monthly sediment for 1994 modeling.

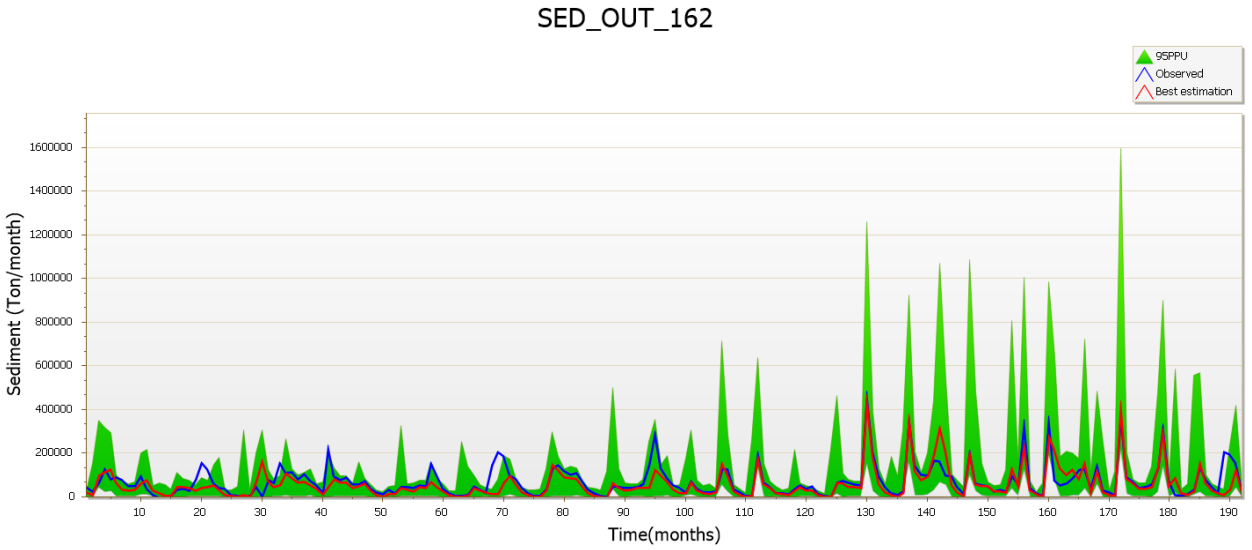

Figure 4.11 Comparison of the observed data with the simulated monthly sediment for 2000 modeling.

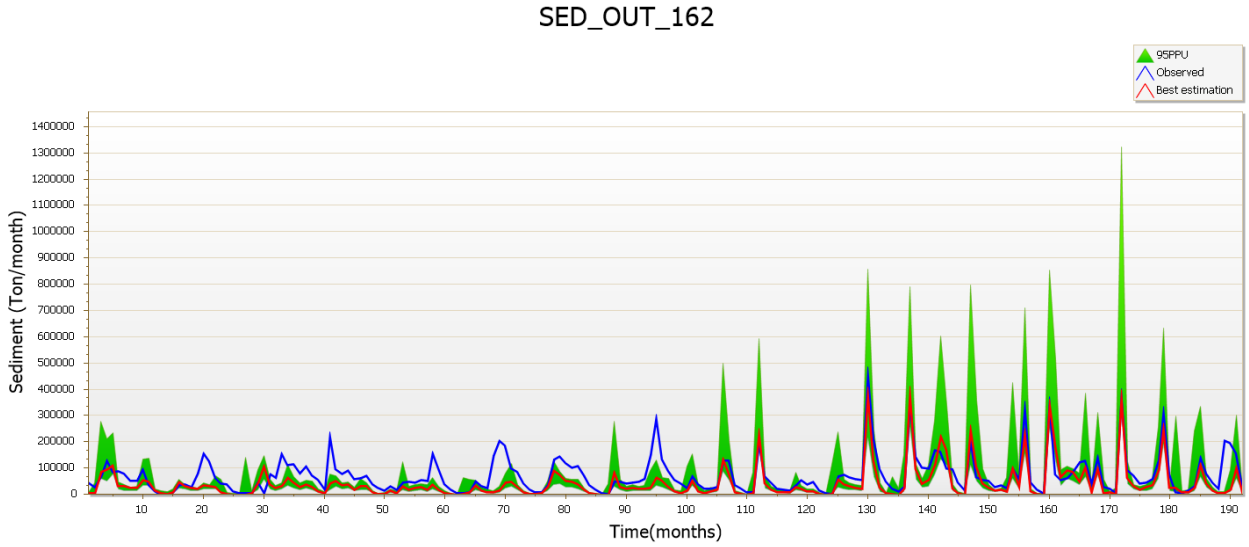

Figure 4.12 Comparison of the observed data with the simulated monthly sediment for 2017

4.4.4. Sediment validation

Similar to flow validation, sediment yield validation was also performed for twelve years from 2004- 2015; which includes two year for model warm up period. Therefore, for the model performance evaluation the validation period was considered from 2006 to 2015 without further adjustment of sediment sensitive parameters. The simulated sediment load versus measured sediment load was compared graphically and statistically. As shown in table 5.11 Coefficient of determination **(**R^2**)** value and Nash-Sutcliffe model efficiency (NSE) are calculated among the predicted and measured monthly sediment yields were 0.64 and 0.56 for modeling of 1994, 0.61 and 0.57 for modeling 2000 and 0.65 and 0.59 respectively.

The measured and simulated sediment yield of monthly time based of a validation period indicates a good agreement, but there was also in certain months under estimation and over estimation. The result of simulated and observed monthly flow of the Chenemesa gauging station was plotted to visualize the degree of certainty (Figure 5.13, Figure 5.14, and Figure 5.15).

Table 4-11Summary of flow sediment validation performance criteria result

performance criteria	1994	2000	2017
R^2	0.64	0.61	0.65
NS	0.56	0.57	0.59

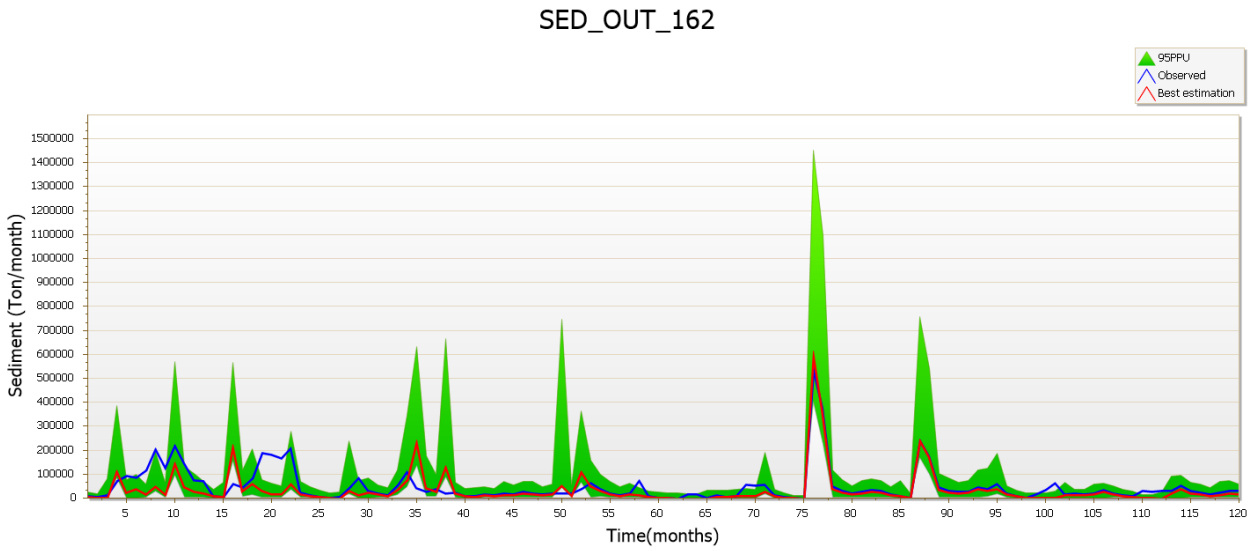

Figure 4.13 Relationship of the observed data with the simulated monthly sediment for 1994 modeling.

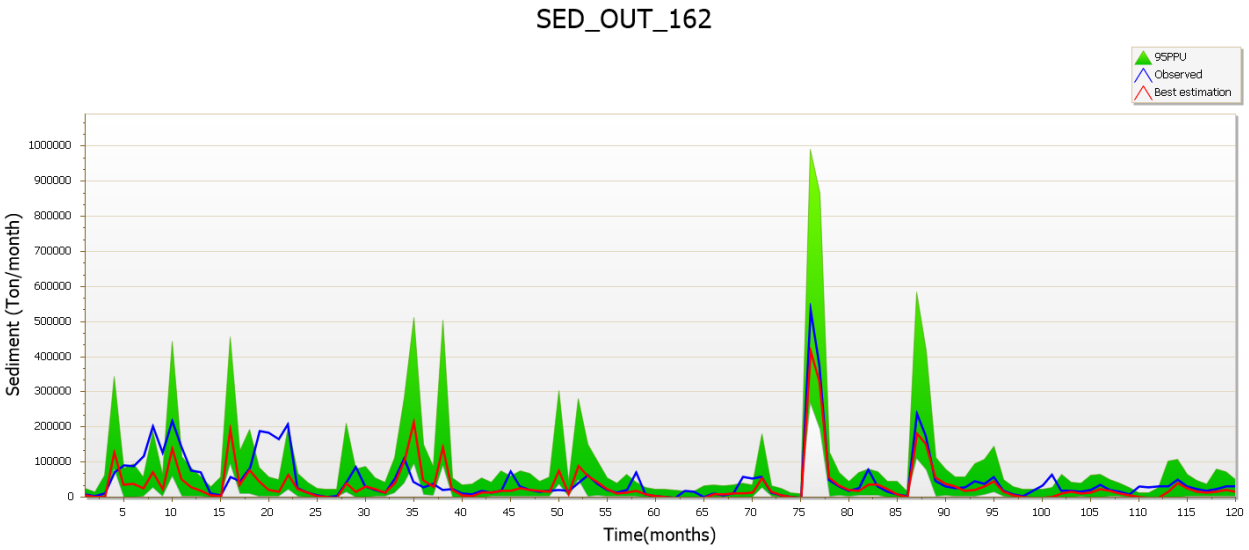

Figure 4.14 Relationship of the observed data with the simulated monthly sediment for 2000 modeling.

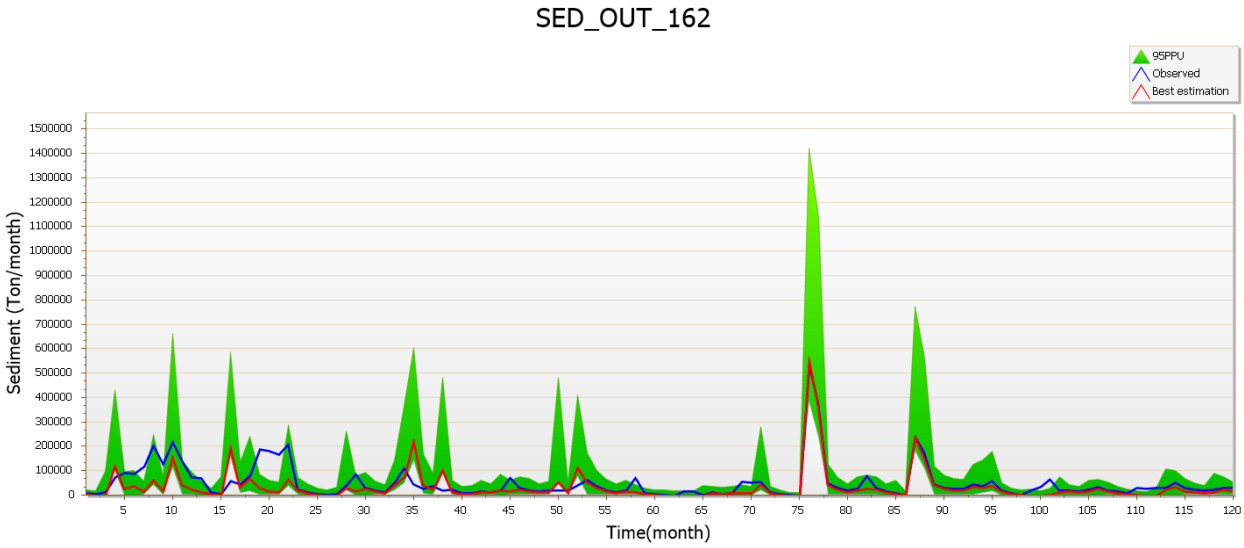

Figure 4.15 Relationship of the observed data with the simulated monthly sediment for 2017

4.5. Effects of land use land cover change on runoff and sediment yield

The impacts of land use land cover change was evaluated by using the calibrated and validated results of models for three periods (1994, 2000, and 2017) using the same DEM, soil, and others data by changing only land use land cover data. As it is shown in the table 5.12 the total amount of average monthly surface runoff in land use land cover 1994, 200 2017 models were 77.8mm,102.2mm, 130.6mm respectively. Similarly the total amount of average monthly sediment yield for the year of 1994, 2000, 2017 it were 14.1t/ha, 16.6t/ha, 24.3t/ha respectively.

Table 4-12 Average monthly runoff for three period LULC (1994, 2000, 2017)

month	runoff (mm)			
	LULC 1994	LULC 2000	LULC 2017	net Variation since1994 to 2017
January	1.2	1.6	2.1	0.9
February	1.8	2.2	2.8	1.0
March	8.2	7.5	5.9	-2.3
April	18.5	23.4	22.5	3.9
May	18.6	21.9	27.8	9.2
June	4.3	3.8	4.9	0.6
July	2.5	2.0	2.6	0.1
August	3.6	2.8	3.7	0.1
September	6.1	5.2	6.9	0.8
October	17.1	17.7	22.8	5.7
November	11.1	9.9	12.7	1.6
December	2.1	2.2	2.9	0.8
total	**95.2**	**100.1**	**117.5**	**22.3**

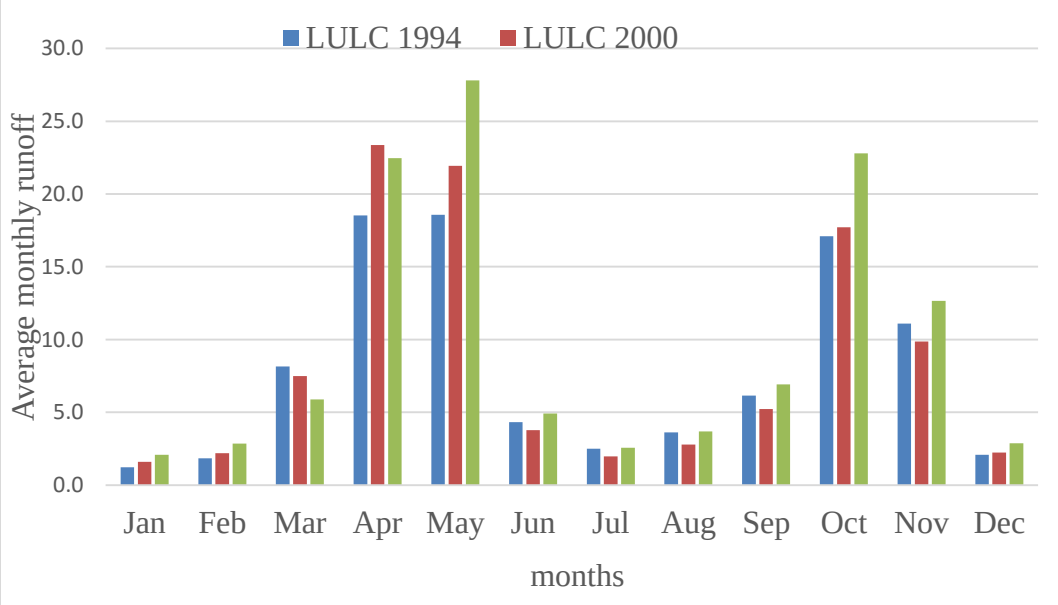

Figure 4.16 Impact of LULC change on runoff

Table 4-13 Average monthly Sediment for three period LULC (1994, 2000, and 2017)

month	sediment yield (t/ha)			
	LULC 1994	LULC 2000	LULC 2017	net Variation since1994 to 2017
January	0.382	0.414	0.558	0.176
February	0.541	0.583	0.776	0.234
March	0.732	1.294	1.983	1.251
April	3.422	3.731	5.583	2.161
May	3.249	3.447	5.276	2.027
June	0.500	0.654	1.115	0.615
July	0.238	0.377	0.589	0.351
August	0.274	0.479	0.736	0.462
September	0.423	0.687	1.018	0.595
October	2.461	2.836	3.885	1.424
November	1.486	1.472	1.956	0.470
December	0.389	0.576	0.776	0.387
Total	**14.1**	**16.6**	**24.3**	**10.2**

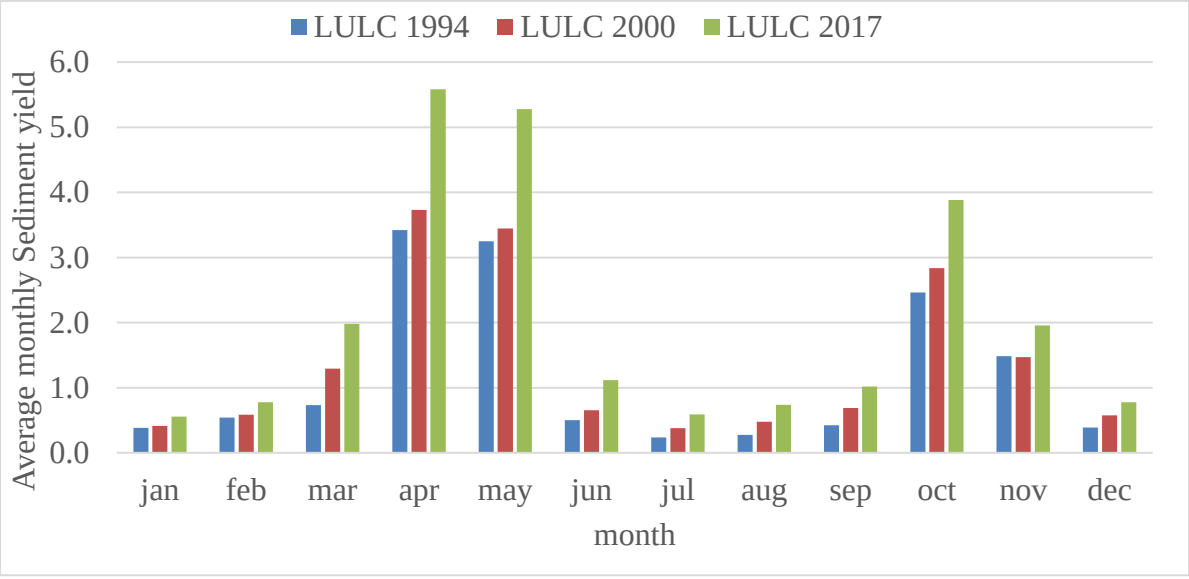

Figure 4.17 Impact of LULC change on sediment yield

4.6. Spatial Variability of Sediment yield

GIS was a tool used to integrate the LULC, slope, soils and river as a key element which has influences for sediment yield production. Different researchers were classifying the soil loss rate in to five categories (Esa, Assen, and Legass 2018). Accordingly Genale sub-basin were reclassified into five main classes of soil erosion region i.e. very low, low, moderate, high and very high. Based on this, the output of swat model has shown that 6.7%, 5.2%, and 11.9% of sub-basin area has very high erosion, 7.3%, 14.0%, and 16.8% high erosion, 18.2%, 19.2%, 26.2% moderate erosion, 32.2%, 23.4%, 25.2% has low erosion, 35.3%, 38.1%, 19.9% potential of soil erosion for land use/cover of 1994, 2000, 2017 respectively (table 5.14). In other ways it has a contribution of average annual sediment yield from each sub-basin ranges from 0.1ton per hectare per year to 129 ton per hectare per year for 1994 LULC, 0.1 ton per hectare per year to 111.1 ton per hectare per year for 2000 LULC and 1 ton per hectare per year to 162.5 ton per hectare per year for 2017LULC during the period from (1990-2017). See (Appendix: 4).

Table 4-14 annual sediment yield severity classes of Ganale sub-basins

rate of sed. yield t/ha/yr	1994		2000		2017		severity
	no. of sub-basin	%	no. of sub-basin	%	no. of sub-basin	%	
0-5	101	35.3	109	38.1	57	19.9	very low
6-15	92	32.2	67	23.4	72	25.2	Low
16-30	52	18.2	55	19.2	75	26.2	Moderate
31-50	21	7.3	40	14.0	48	16.8	high
50+	20	7.0	15	5.2	34	11.9	very high

But according to (Harni 1983) the limit of an acceptable soil loss for many agricultural ecosystem of Ethiopia was found from 2 ton/ha to 18 ton/ha. According to this ranges the output of the three swat model (1994, 2000, and 2017) shows that 29.02 %, 31.1 %, 49.3 % of the sub-basins has above tolerable soil rate erosion and about 71.0%, 69.0%, 50.7% of the sub-basins are below or in recommended (tolerable) soil loss rate respectively. The spatial variability of average sediment yield that generated from Ganale sub-basin were represented in Figure (5.19), Figure (5.20)and Figure (5.21) which is used to identify the sub-basin that are producing sediment yield.

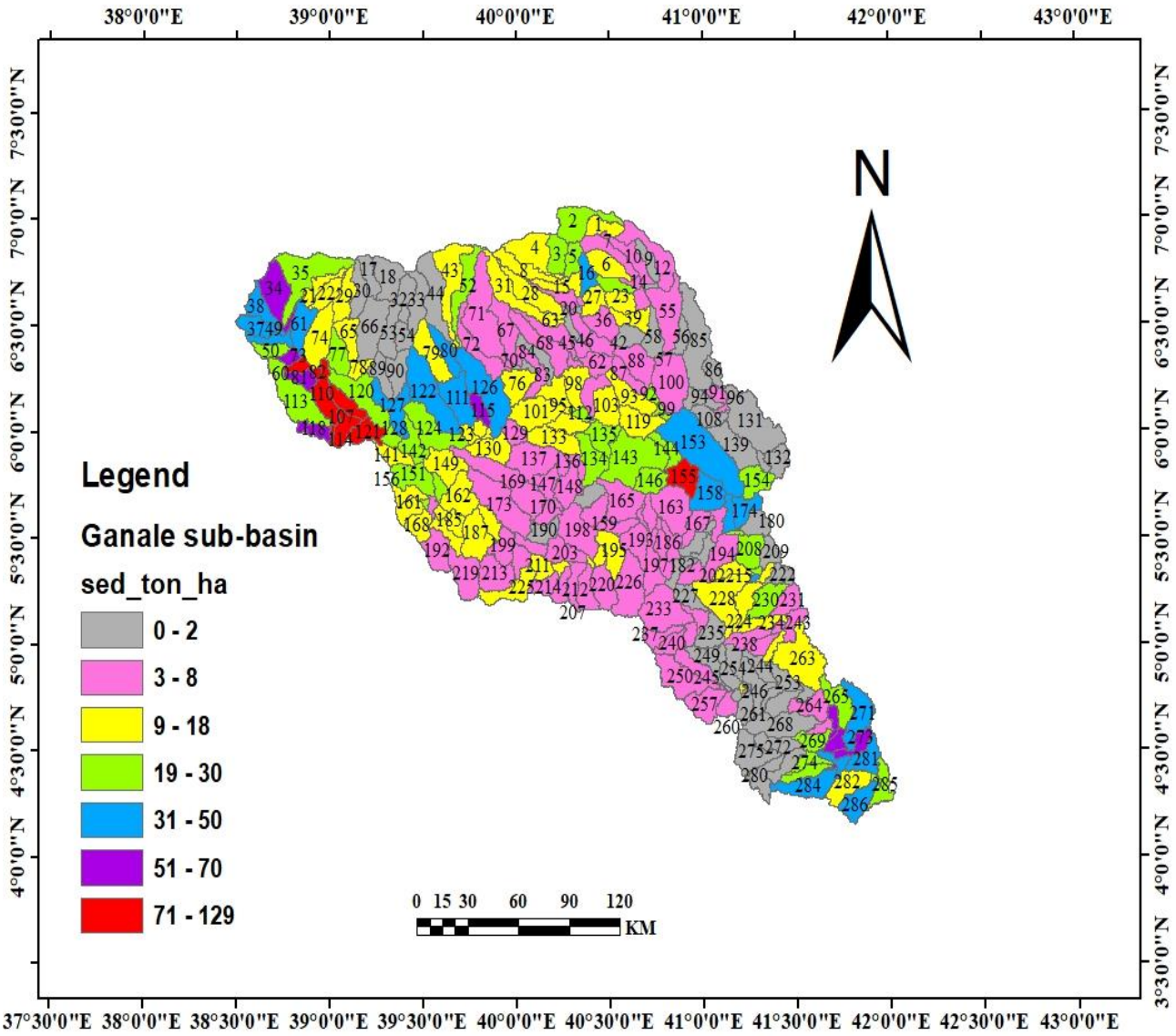

Figure 4.18 Sub-basins sediment yield variability map in the Ganale sub-basin for 1994

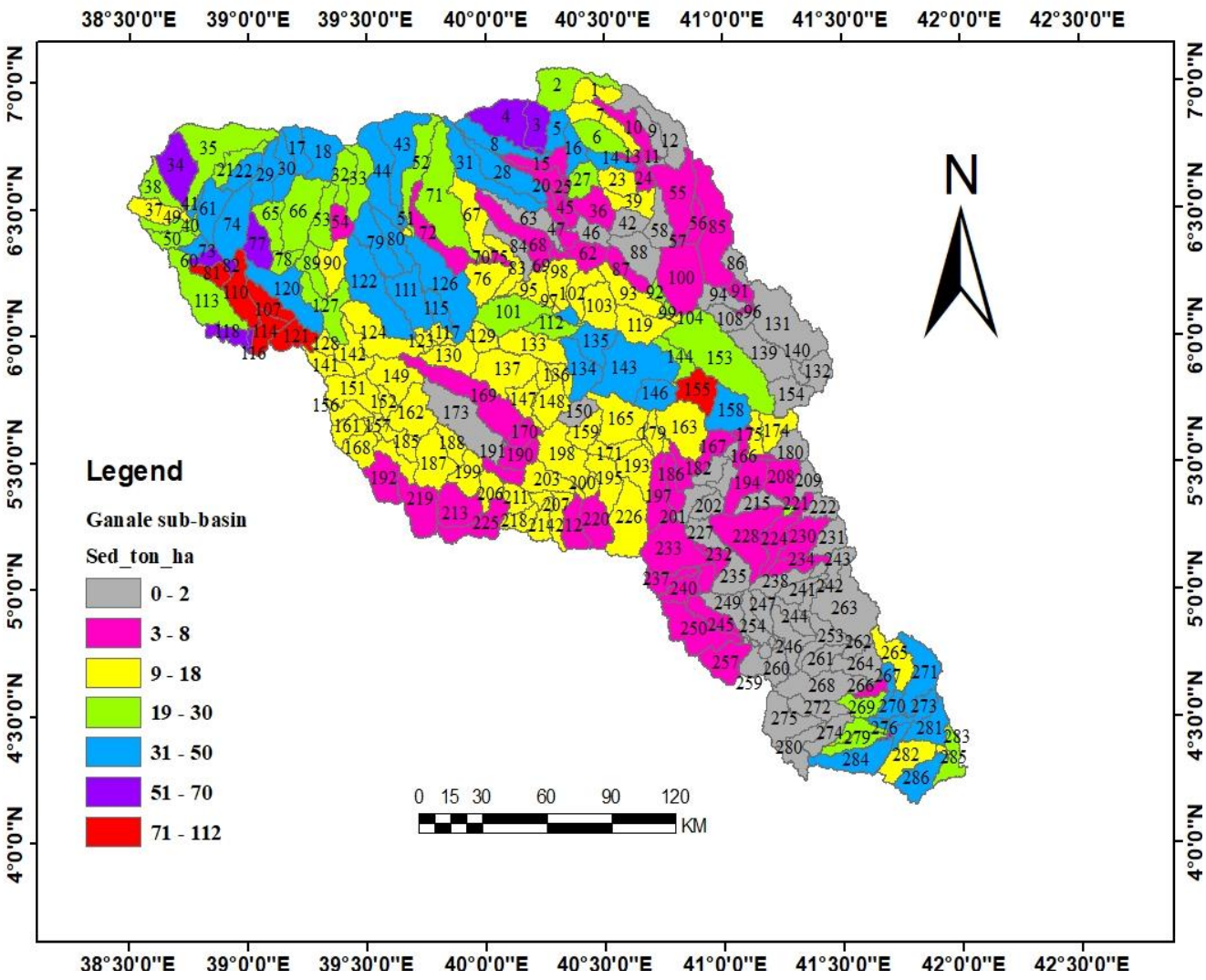

Figure 4.19 Sub-basins sediment yield variability map in the Ganale sub-basin for 2000

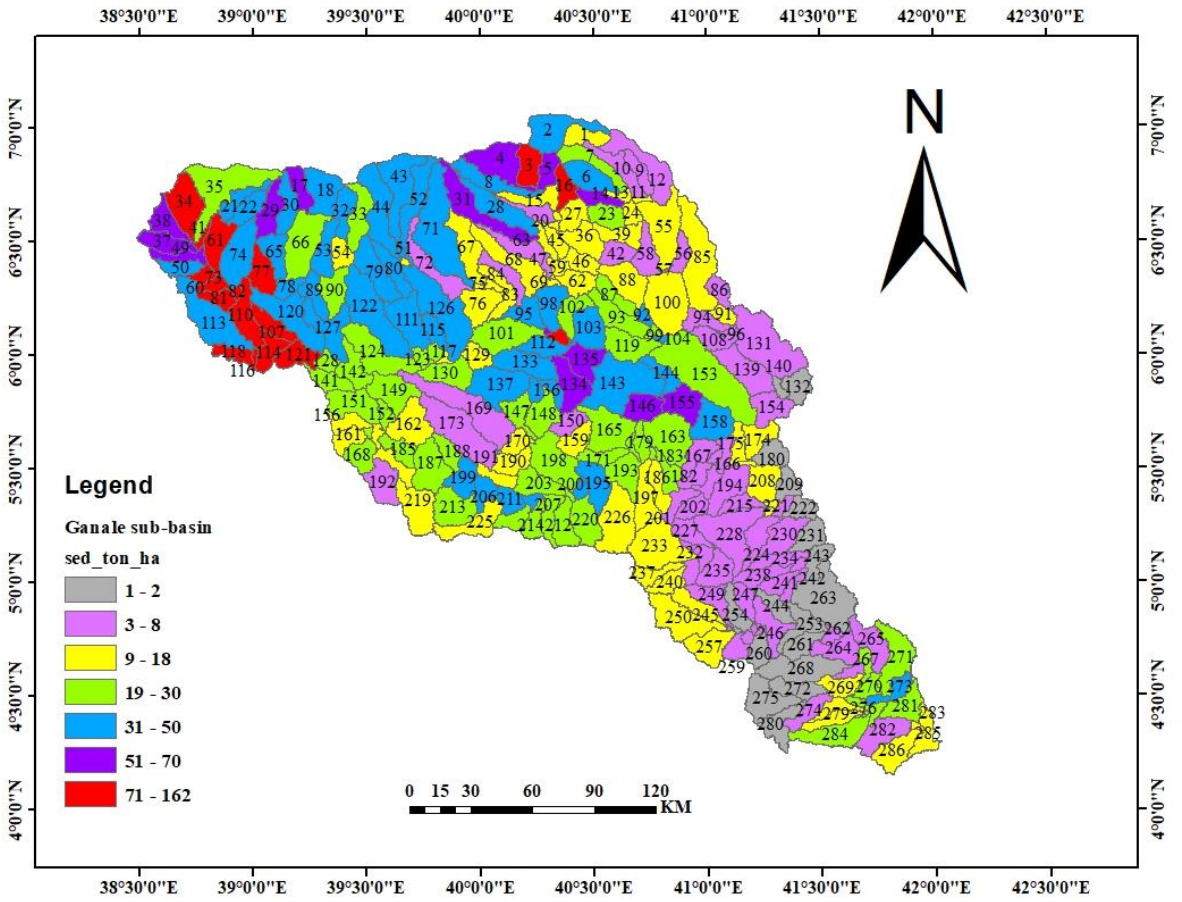

Figure 4.20 Sub-basins sediment yield variability map in the Ganale sub-basin for 2017

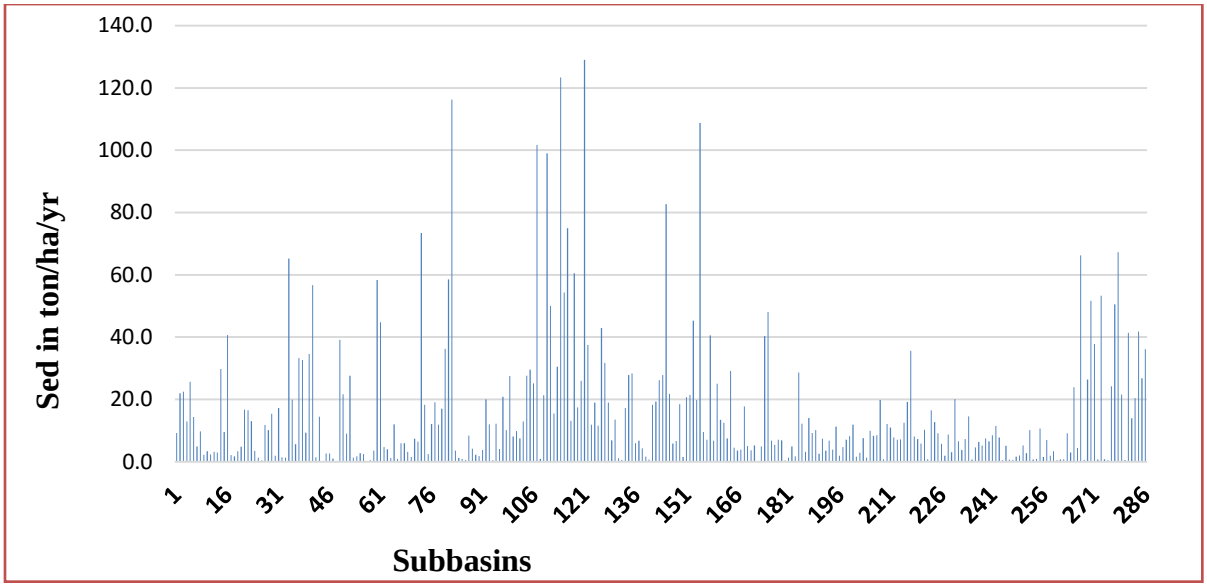

Figure 4.21 SWAT simulated average annual sediment yield distribution of sub basins for 1994

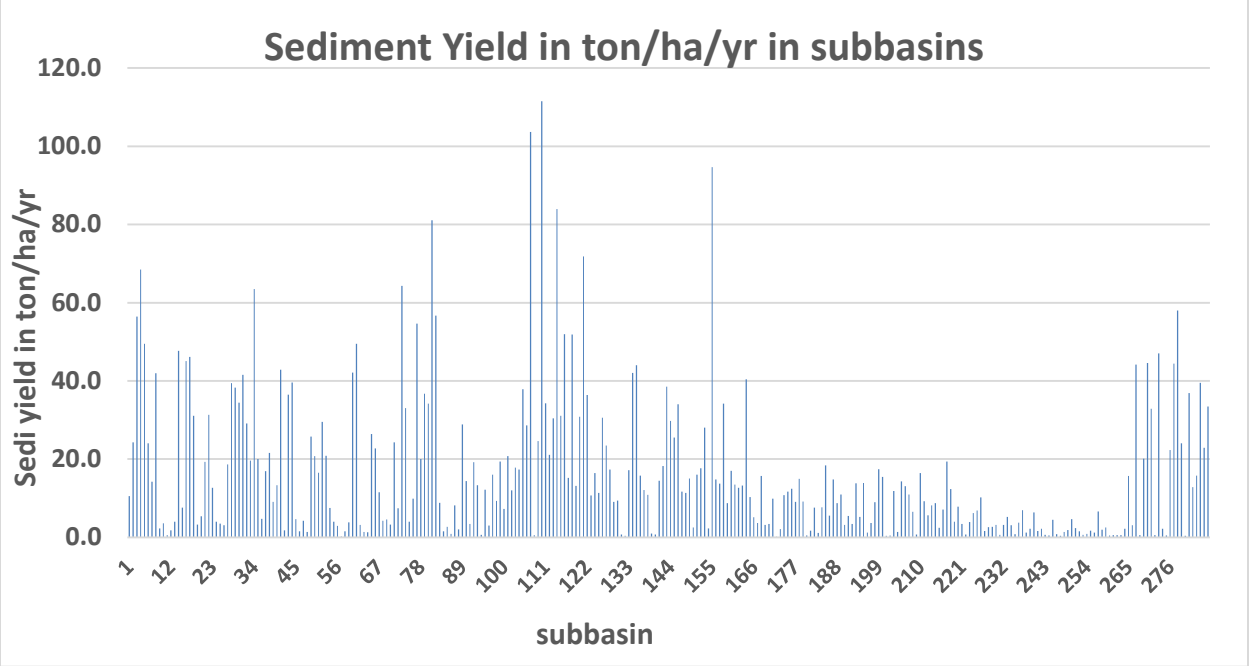

Figure 4.22 SWAT simulated average annual sediment yield distribution of sub basins for 2000

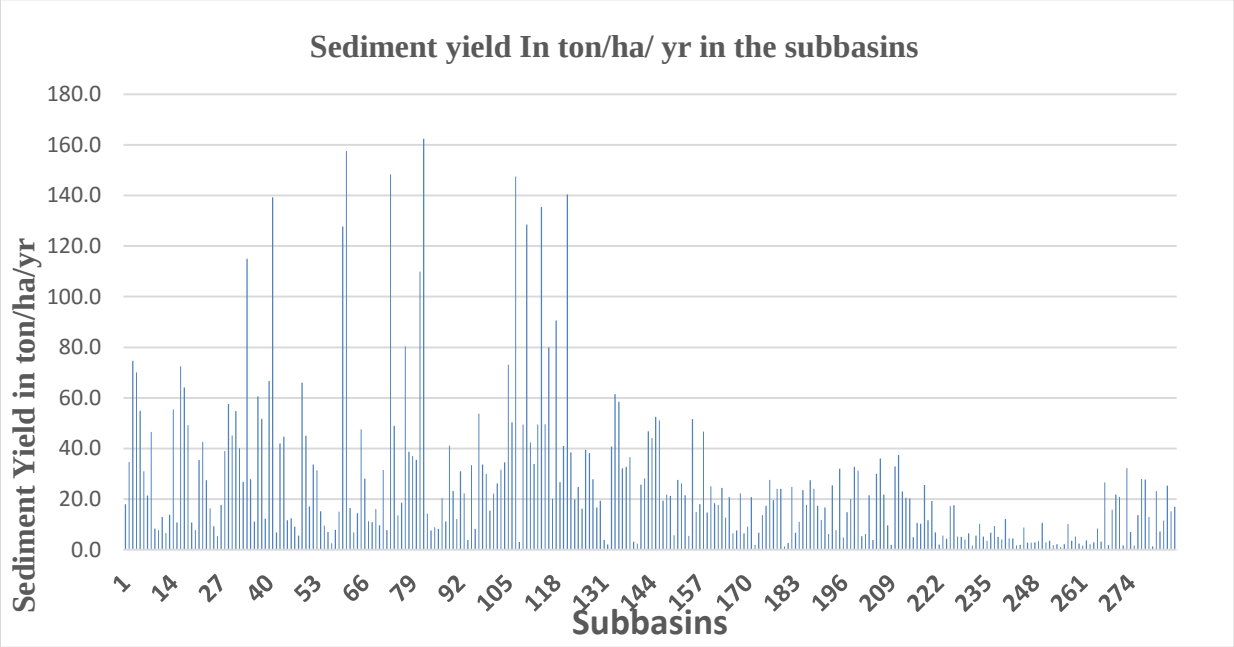

Figure 4.23 SWAT simulated average annual sediment yield distribution of sub basins for 2017

CHAPTER FIVE

5. CONCLUSION AND RECOMMENDATION

5.1. CONCLUSION

The key intention of the research was for examining of the effect of LULC change on Genale Dawa dam_3 reservoir. Within this to classify, assess/evaluate the land use land cover, and estimate runoff and sediment yield under different land use scenarios. Also it was to assess and evaluate the spatial variability of sediment yield and detect the exposed sub-basin for erosion and sediment yield in the Ganale sub-basin.

In this study an integrated approach of Arc-GIS 10.4.1 and ERDAS 2014 with the hydrological model was used to assess the influences of land use LULC change which was the excellent tools for maping different land cover classes, to discover and analyses the spatiotemporal land cover change. The land use land cover changes in Ganale sub-basin of the year 1994, 2000, and 2017 were identified from TM, ETM+, ETM+ satellite images respectively by using ERDAS 2014 and google earth pro.

The identification of sensitive parameters helps to save time during calibration and validation in swat cup program. The most sensitive for the Ganale sub-basin are; ground water parameter (ALPHA_BF, RCHRG_DP.) and the soil properties (ESCO, CH_K1, CH_K2, SOL_Z, SOL_AWC and SOL_K) and curve number for stream flow. Similarly for sediment CH_N2, CN2, USLE_K, SOL_Z, ESCO, ALPHA_BF, EPCO, and SOL_AWC) were the main sensitive parameters that governs sediment calibration.

The SWAT model performance was evaluated by calibration and validation using SWAT CUP software sufi2 program. As the result showed that the reliable estimates of average monthly flow with the acceptable coefficient of determination (R^2) and Nash-Sutcliffe (NS) for the period of calibration and validation. The coefficient of determination (R^2) and Nash-Sutcliffe (NS) value of the stream flow and sediment yield was within the recommended range or good for calibration and validation for all land use land cover modeling.

As shown from the land use/cover analysis in Ganale sub-basin land use/cover has been significantly changed within 24 years (1994 to 2017). From this study it is concluded that the land use/cover map in 1994 the cultivated land coverage was 12.44% and highly increased in 2017 to 40.46%. This is due to decreasing of forest, wood land and grassland coverage for the reason of increasing of new cultivation area and deforestation of wood land and forest. In general grass land, wood land, forest land and bare land use/cover are decreasing whereas cultivation, and bush land are increasing in its coverage area. This may be because of the increase of population for high demand as a consequence a shortage of land and increase of government farm in the study area. And finally this were causes the increase of total average monthly runoff and sediment yield from 77.8mm to130.6mm and 14.1t/ha to 24.3t/ha for the period of1994 to 2017 respectively. In year of 1994 the total average monthly runoff and sediment yield was 77.8mm and 14.1t/ha, in 2000 it was 102.2mm and 16.6t/ha, and in 2017 it was 130.6mm.

The model were calibrated from 1990 to 2005 and validated from 2006 to 2015 on monthly basis at the sub-basin scale and had the capability to identify the areas of high erosion and sediment yield. Hence, the model prediction verified that for 1994, 2000, 2017 LULC about 29.02 %, 31.1 %, 49.3 % of sub-basin has very high erosion potential area to contribute high sediment yield exceeding the tolerable limit in the study area and about 71.0%, 69.0%, 50.7% of sub-basin high erosion potential for soil erosion which produce above annual average sediment yield of the sub-basin respectively. Therefore, the spatial distribution of soil loss rate obtained from this investigation is helpful in prioritizing areas that needs immediate mitigation measures to reduce soil erosion.

5.2. Recommendation

- Soil and watershed management conservation practices are highly recommended to safe these severe erosion parts and the concerned body should work closely with the stockholders living in the study areas.
- Further researches on sedimentation effects on reservoir can be suggested by using different scenarios.
- The reliability and availability of data is a primary point for any studies and responsible body should take of data quality and quantity for sediment, flow and weather data for future studies.

References

Abbaspour, K. C. 2014. “SWAT-CUP 2012: SWAT Calibration and Uncertainty Programs - A User Manual.” *Science And Technology*, 106. https://doi.org/10.1007/s00402-009-1032-4.

Abby, P, J Forrer, C Steinmeier, and H Fluhler. 1997. “DIVISION S-l-NOTES” 35: 33–35.

Ahmed, Hussein. 2006. “Addis Ababa University.” *Cahiers d’études Africaines* 46 (182): 291–312. https://doi.org/10.4000/etudesafricaines.5928.

Asmerom, Tilahun Araya. 2015. “Assessing Surface Water Potential and Water Demand in Genale Dawa River Basin A Thesis Submitted in Partial Fulfillment of the Requirements for the Degree of Master of Science in Hydraulic Engineering School of Civil and Environmental Engineering Addis Ab.”

Bewket, W. 2003. “Towards Integrated Watershed Management in Highland Ethiopia: The Chemoga Watershed Case Study.” *Towards Integrated Watershed Management in Highland Ethiopia: The Chemoga Watershed Case Study*, 169–pp.

Bewket, Woldeamlak, and Geert Sterk. 2005. “Dynamics in Land Cover and Its Effect on Stream Flow in the Chemoga Watershed, Blue Nile Basin, Ethiopia.” *Hydrological Processes* 19 (2): 445–58. https://doi.org/10.1002/hyp.5542.

Croke, B. F.W., W. S. Merritt, and A. J. Jakeman. 2004. “A Dynamic Model for Predicting Hydrologic Response to Land Cover Changes in Gauged and Ungauged Catchments.” *Journal of Hydrology* 291 (1–2): 115–31. https://doi.org/10.1016/j.jhydrol.2003.12.012.

Cunderlik. 2003. “Assessment of Water Resources Risk and Vulnerability to Changing Climatic Conditions.”

Esa, Ebrahim, Mohammed Assen, and Asmamaw Legass. 2018. “Implications of Land Use/Cover Dynamics on Soil Erosion Potential of Agricultural Watershed, Northwestern Highlands of Ethiopia.” *Environmental Systems Research* 7 (1). https://doi.org/10.1186/s40068-018-0122-0.

Gassman, Philip W., Manuel R. Reyes, Colleen H. Green, and Jeffrey G. Arnold. 2007. “The Soil and Water Assessment Tool: Historical Development, Applications, and Future Research Directions.” *Transactions of the ASABE* 50 (4): 1211–50.

Gassman, Philip W, and Manuel Reyes. 2016. “SWAT Peer-Reviewed Literature : A Review by • SWAT History : Key Model Development.” *Soil and Water*.

GDMP. 2007. “The Federal Democratic Republic of Ethiopia Genale-Dawa River Basin

Integrated Resources Development Master Plan Genale (GD-3) Multipurpose Hydropower Project" IV (August).

Gemechu, Teka. 2014. "Estimating the Impacts of Land Use and Land Cover Change on Runoff and Sediment Yield Using SWAT Model : Case Study of Keleta Watershed , Upper Awash Sub-Basin," no. January.

Harni. 1983. "Soil Formation Rates in Ethiopia EHRS." *The Geographical Journal* 101 (1): 1. https://doi.org/10.2307/1790117.

Hietel, Elke, Rainer Waldhardt, and Annette Otte. 2004. "Analysing Land-Cover Changes in Relation to Environmental Variables in Hesse, Germany." *Landscape Ecology* 19 (5): 473–89. https://doi.org/10.1023/B:LAND.0000036138.82213.80.

Ibrahim. 2018. "Mpact of Land Use Dynamics on Reservior Sedimentation in Megech Watershed , Upper Blue Nile , Ethiopia By Addis Ababa," no. June.

Klein Goldewijk, Kees, and Navin Ramankutty. 2004. "Land Cover Change over the Last Three Centuries Due to Human Activities: The Availability of New Global Data Sets." *GeoJournal* 61 (4): 335–44. https://doi.org/10.1007/s10708-004-5050-z.

Lemenkova, Polina. 2015. *Processing Remote Sensing Data Using Erdas Imagine for Mapping Aegean Sea Region, Turkey*. https://doi.org/10.6084/m9.figshare.7434191.

Lenhart. 2002. "Comparison of Two Different Approaches for Making Design Sensitivity Analysis an Integrated Part of Finite Element Analysis." *Structural Optimization* 3 (3): 149–56. https://doi.org/10.1007/BF01743071.

McNeil, J, D Alves, L Arizpa, O Bykova, K Galvin, J Kelmelis, S Migot-Adholla, et al. 1994. "Toward a Typoligy and Regionalization of Land Cover and Land Use Change." *Changes in Land Use and Land Cover: A Global Perspective* GF3 (33): 55–72. http://mtc-m12.sid.inpe.br/col/sid.inpe.br/iris@1912/2005/07.20.05.00/doc/INPE 6541.pdf.

Morris, By Gregory L, and Jiahau Fan. 2000. "R s h —d m w s U," no. June: 481–82.

Nash, Sutcliffe. 1970. "Ireland's Water Budget - Model Validation and a Greenhouse Experiment." *Irish Geography* 34 (2): 124–34. https://doi.org/10.1080/00750770109555783.

Seifu. 2015. "Runoff and Sediment Yield Estimation Using Swat Model (A Case Study Of Upper Dabus Watershed, Abbay Basin, Ethiopia)."

Shimelis G. Setegn, 1, 2* Ragahavan Srinivasan, 3 Bijan Dargahi1 and Assefa M. Melesse2.

2010. “Advanced Bash-Scripting Guide An in-Depth Exploration of the Art of Shell Scripting Table of Contents.” *Okt 2005 Abrufbar Uber Httpwww Tldp OrgLDPabsabsguide Pdf Zugriff 1112 2005* 2274 (November 2008): 2267–74. https://doi.org/10.1002/hyp.

Tesfahunegn, Gebreyesus Brhane, Paul L.G. Vlek, and Lulseged Tamene. 2012. “Management Strategies for Reducing Soil Degradation through Modeling in a GIS Environment in Northern Ethiopia Catchment.” *Nutrient Cycling in Agroecosystems* 92 (3): 255–72. https://doi.org/10.1007/s10705-012-9488-y.

Victor, David G, and Jesse H Ausubel. 2000. “FOREIGN AFFAIRS Restoring the Forests” 79 (6).

White, Kati L., and Indrajeet Chaubey. 2005. “Sensitivity Analysis, Calibration, and Validations for a Multisite and Multivariable SWAT Model.” *Journal of the American Water Resources Association* 41 (5): 1077–89. https://doi.org/10.1111/j.1752-1688.2005.tb03786.x.

Xiuwan, Chen. 2002. “Using Remote Sensing and GIS to Analyse Land Cover Change and Its Impacts on Regional Sustainable Development.” *International Journal of Remote Sensing* 23 (1): 107–24. https://doi.org/10.1080/01431160010007051.

Zheng, C., M. C. Hill, G. Cao, and R. Ma. 2012. “MT3DMS: Model Use, Calibration, and Validation.” *Transactions of the ASABE* 55 (4): 1549–59.

Bewket, W. (2003). Towards integrated watershed management in highland ethiopia: the Chemoga watershed case study, PhD thesis, Wageningen University and Research Centre, ISBN 90-5808-870-7.

Belay, T. (2002). Land cover/use changes in the Derekolli catchment of the South Welo Zone of Amhara Region, Ethiopia. Eastern Africa Social Science Research Review 18(1): 1-20.

Abebe, S. (2005). Land-Use and Land-Cover change in headstream of Abbay watershed, Blue Nile Basin, Ethiopia. Addis Ababa University.

Denboba, M. (2005). Forest conversion-soil degradation-farmers' perception nexus: Implications for sustainable land use in the southwest of Ethiopia. Ecology and Development Series No. 26, 2005.

Garedew, E. (2010). Land-Use and Land-Cover dynamics and rural livelihood perspectives, in the semiarid areas of the central Rift Valley of Ethiopia, PhD thesis, Swedish University

of Agricultural Sciences.

Gebrehiwet, K. (2004). Land use and land cover changes in the central highlands of Ethiopia: The case of Yerer mountain and its surroundings. M.Sc Thesis, Addis Ababa University, Environmental Science.

Hadgu, K. (2008). Temporal and spatial changes in land use patterns and biodiversity in relation to farm productivity at multiple scales in Tigray, Ethiopia. PhD Thesis Wageningen University, Wageningen, the Netherlands

Kassa, G. (2003). GIS based analysis of land use and land cover, land degradation and population changes: A study of Boru Metero area of south Wello, Amhara Region, MA Thesis, Department of Geology, Addis Ababa University. 110pp

APPENDICES

Appendix: 1 Average monthly stream flow at Chenemesa gauging Station for (1988-2015).

year/ month	Jan	Feb	Mar	Apr	May	Jun	Jul	Aug	Sep	Oct	Nov	Dec	Annual mean
1988	10.8	5.3	4.6	22.2	56.3	62.0	161.0	228.9	154.0	296.6	63.0	14.6	90.6
1989	6.4	4.9	5.7	99.4	68.8	88.9	135.4	135.1	270.8	313.1	122.2	139.6	116.4
1990	43.8	109.7	151.3	322.4	313.9	254.6	173.1	177.1	146.5	218.0	183.5	103.7	99.4
1991	61.5	48.2	169.6	191.9	216.8	155.8	145.4	230.5	270.8	313.1	122.2	46.9	66.1
1992	25.1	22.3	33.4	147.6	331.2	318.9	185.3	202.0	204.4	361.2	203.2	247.5	102.0
1993	68.6	131.3	86.8	86.8	246.1	91.7	74.2	134.6	118.1	215.2	125.7	42.3	118.5
1994	20.6	18.8	23.1	42.7	147.8	143.5	202.3	258.0	171.1	179.8	122.4	59.8	116.6
1995	32.2	27.5	46.1	133.8	113.9	61.5	88.2	164.4	227.5	203.1	86.0	22.4	100.9
1996	17.1	12.8	7.5	50.5	138.5	278.8	156.2	196.9	239.6	126.8	38.4	16.1	106.6
1997	10.2	5.0	1.6	40.9	44.5	41.7	117.2	102.9	63.9	249.9	481.2	168.1	111.0
1998	181.2	113.2	50.1	49.7	139.5	66.2	133.1	192.9	187.3	351.1	118.8	27.3	134.7
1999	12.7	4.8	12.2	14.1	36.2	37.1	98.4	127.5	118.5	248.2	89.9	20.1	68.9
2000	4.8	1.1	0.2	4.8	122.7	28.8	60.0	140.8	148.9	259.9	203.6	42.8	85.2
2001	13.2	9.6	14.8	45.2	120.0	163.9	138.4	189.7	197.7	181.5	120.8	41.9	103.5
2002	22.7	9.6	20.5	40.6	56.5	45.6	71.1	110.3	93.9	108.5	48.5	48.2	56.7
2003	36.5	10.8	7.5	47.4	92.2	75.6	81.7	106.6	117.5	115.2	47.5	54.3	66.4
2004	34.6	26.9	10.8	41.2	64.8	53.7	67.5	141.4	178.5	163.6	87.5	40.3	76.0
2005	18.2	11.6	25.5	44.9	276.9	105.5	111.5	172.1	228.3	213.1	178.5	45.7	120.0
2006	16.1	11.8	20.7	92.8	111.5	110.7	136.1	222.3	154.2	228.2	167.2	94.3	114.5
2007	89.7	23.4	17.7	78.2	95.7	257.5	205.8	201.7	191.4	224.5	82.8	21.7	124.7
2008	15.2	9.5	10.8	13.0	105.6	53.6	39.4	84.6	89.1	94.7	60.9	42.4	51.8
2009	35.4	34.5	30.8	35.4	35.3	31.9	48.3	70.1	97.5	44.4	39.3	38.1	45.1
2010	36.6	36.5	41.2	57.7	111.6	63.5	49.4	44.1	76.5	94.0	51.7	31.5	58.0
2011	28.8	28.7	28.4	28.1	46.6	86.4	53.3	59.0	77.9	70.8	74.1	42.5	52.1
2012	26.5	0.5	0.4	1.6	5.2	56.2	47.1	55.4	72.8	101.6	62.4	29.9	38.4
2013	27.2	27.1	40.1	56.4	83.5	63.1	47.8	49.7	57.1	72.7	32.4	28.0	48.9
2014	36.3	36.4	29.5	50.9	84.6	60.7	70.6	101.2	79.5	141.3	66.0	45.7	67.2
2015	45.9	46.0	46.1	46.1	46.1	46.1	46.1	45.9	45.9	46.0	46.2	46.4	46.0

Appendix 2 observed sediment concentration at Chenemesa station

date of sampling	FLOW	Sediment Concentration in(mg/l)
17-Oct-89	228.55	204
20-Oct-89	565.17	482
19-Oct-89	486.74	722
18-Oct-89	142.154	291
4-Apr-90	355.6535	309
13-Apr-90	184.13	262
27-May-96	133.091	331
12-Aug-96	158.6105	215
8-Mar-96	204.66	89
19-Sep-97	146.974	131
28-May-03	10.76	356
28-May-03	120.798	355
9-Dec-04	48.015	138
30-Dec-04	48.36	189
14-Jan-05	54.78	56
27-Jan-05	34.37	100
14-Feb-05	44.575	97
26-Feb-05	14.88	108
12-Mar-05	9.92	219
6-Apr-05	8.95	143
2-Apr-05	5.1	297
5-May-05	20.02	1803
15-May-05	9.96	661
17-May-05	56.66	695
18-May-05	189.82	6217
19-May-05	266.91	2127
20-May-05	298.23	2513
21-May-05	241.06	1057
22-May-05	98.04	1822
28-May-05	92.96	1352
13-Jul-05	176.8	220
14-Jul-05	125.1	174
29-Jul-05	162.51	491
9-Aug-05	374.98	248
26-Aug-05	159.44	545
18-Sep-05	148.24	1627
1-Oct-05	158.21	398
20-Oct-05	169.5	290
21-Oct-05	144.26	304

22-Oct-05	103.65	293
24-Oct-05	0.82	432
13-Nov-05	86.07	144
24-Sep-05	36.62	322
27-Nov-05	121.4888	150
16-Dec-05	163.003	138
21-Sep-07	154.248	307
22-Sep-07	139.301	251
23-Sep-07	163.974	197
24-Sep-07	176.24	234
26-Sep-07	196.138	287
27-Sep-07	224.671	393
28-Sep-07	222.087	610
29-Sep-07	280.354	346
1-Oct-07	372.07	678
2-Oct-07	454.573	524
4-Oct-07	338.932	575
6-Oct-07	283.171	330
7-Oct-07	194.585	413
9-Oct-07	175.124	386
11-Oct-07	126.134	323
14-Oct-07	194.061	257
16-Oct-07	152.922	398
19-Oct-07	229.74	260
21-Oct-07	241.465	493
23-Oct-07	183.674	413
25-Oct-07	143.324	342
28-Oct-07	105.053	331
31-Oct-07	96.035	209
2-Nov-07	80.79	211
4-Nov-07	89.085	162
6-Nov-07	74.696	155
8-Nov-07	194.6463	158
18-Sep-10	185.358	549
30-Sep-14	1.26	1062
2-Oct-14	1.14	260

Appendix 3 Soil physiochemical and textural characteristics of the study area used in the SWAT model.

SOIL NAME	CMPPCT	NLAYERS	HYDGRP	SOL_ZMX	ANION_EXCL	SOL_CRK	TEXTURE	SOL_Z	SOL_BD	SOL_AWC	SOL_K	SOL_CBN	CLAY	SILT	SAND	ROCK	SOL_ALB	USLE_K
CMARENOSOLS		1	A	1000	0.50	0.50	Sand	100	1.7	0.1	360	0.5	5	6	89	2	0.374	0.158116
		2						200	1.4	0.124	4.43	0.9	26	42	32	0	0.0863	0.3069
		3						1000	1.4	0.124	4.14	0.5	31	36	33	0	0.1867	0.3069
HPCALCISOLS		1	A	1000	0.50	0.50	Sand	100	1.6	0.1	360	0.4	9	10	81	10	0.226	0.153456
		2						200	1.4	0.048	4.59	0.8	25	42	33	0	0.1047	0.3267
		3						1000	1.5	0.048	2.5	0.5	30	37	33	0	0.1867	0.3267
PTCALCISOLS		1	A	1000	0.50	0.50	Sand	100	1.61	0.1	360	0.4	9	8	83	28	0.226	0.149016
		2						200	1.4	0.056	4.96	0.7	23	45	32	0	0.1269	0.3482
		3						1000	1.4	0.056	4.53	0.4	25	36	38	0	0.2265	0.3482
EUCAMBISOLS		1	D	1000	0.50	0.50	Sand	100	1.25	0.05	0.00036	1.17	48	29	23	10	0.226	0.134617
		2						200	1.3	0.16	8.03	1.2	24	46	30	0	0.0484	0.2759
		3						1000	1.3	0.16	7	0.6	30	43	26	0	0.154	0.2759
CHCAMBISOLS		1	D	1000	0.50	0.50	Sand	100	1.24	0.15	0.00036	1.43	50	29	21	2	0.226	0.126115
		2						200	1.3	0.16	8.03	1.2	24	46	30	0	0.0484	0.2759
		3						1000	1.3	0.16	7	0.6	30	43	26	0	0.154	0.2759
CLFLUVISOLS		1	A	1000	0.50	0.50	Sand	100	1.66	0.15	360	0.41	6	15	79	10	0.321	0.167808
		2						200	1.5	0.175	2.34	0.9	32	39	28	0	0.0863	0.353
		3						1000	1.4	0.175	3.92	0.4	34	41	25	0	0.2265	0.353
HPGYPSISOLS		1	B	1000	0.50	0.50	Sand	100	1.37	0.15	18	0.47	24	40	36	2	0.226	0.172819
		2						200	1.4	0.056	4.96	0.7	23	45	32	0	0.1269	0.3482
		3						1000	1.4	0.056	4.53	0.4	25	36	38	0	0.2265	0.3482
PTGYPSISOLS		1	A	1000	0.50	0.50	Sand	100	1.66	0.1	360	0.53	6	13	81	10	0.226	0.164885
		2						200	1.4	0.158	9.51	0.5	17	32	50	0	0.1867	0.3498
		3						1000	1.3	0.158	9.17	0.3	20	43	36	0	0.2747	0.3498
EULEPTOSOLS		1	A	1000	0.50	0.50	Sand	30	1.61	0.015	180	0.6	8	16	76	20	0.226	0.16299
		2						100	1.1	0.17	23.56	0.7	43	28	29	0	0.1269	0.26
		3						1000	1.3	0.17	8.46	0.4	46	28	26	0	0.2265	0.26
RNLEPTOSOLS		1	A	1000	0.50	0.50	Sand	30	1.61	0.05	180	1.93	8	16	76	21	0.211	0.127486
		2						100	1.5	0.175	2.26	0.5	34	43	23	0	0.1867	0.3339
		3						1000	1.4	0.175	3.87	0.3	40	42	18	0	0.2747	0.3339
LTLEPTOSOLS		1	A	1000	0.50	0.50	Sand	10	1.59	0.05	180	1.4	9	18	73	21	0.226	0.139526
		2						50	1.2	0.098	18.76	1.6	26	22	52	0	0.0224	0.2814
		3						1000	1.3	0.098	13.01	0.9	26	21	52	0	0.0863	0.2814
HPLUVISOLS		1	B	1000	0.50	0.50	Sand	100	1.4	0.15	18	0.74	22	37	41	4	0.198	0.168222
		2						200	1.1	0.17	23.56	0.7	43	28	29	0	0.1269	0.26
		3						1000	1.3	0.17	8.46	0.4	46	28	26	0	0.2265	0.26
CHLUVISOLS		1	B	1000	0.50	0.50	Sand	100	1.4	0.15	18	0.83	24	28	48	12	0.198	0.158201
		2						200	1.3	0.15	8.51	1.1	43	28	29	0	0.0587	0.2385
		3						1000	1.2	0.15	12.53	0.5	54	23	23	0	0.1867	0.2385
HUNITISOLS		1	B	1000	0.50	0.50	Sand	100	1.39	0.15	18	2.25	24	31	45	9	0.226	0.127311
		2						200	1.1	0.085	22.04	2.8	36	26	37	0	0.0022	0.2687
		3						1000	1.2	0.085	13.23	1	37	29	35	0	0.0712	0.2687
HPSOLONCHAKS		1	B	1000	0.50	0.50	Sand	100	1.36	0.15	18	0.46	25	41	34	7	0.306	0.173091
		2						0	0	0	0	0	0	0	0	0	0	0
		3						0	0	0	0	0	0	0	0	0	0	0
EUVERTISOLS		1	D	1000	0.50	0.50	Sand	100	1.22	0.125	0.00036	1.05	56	25	19	4	0.231	0.132894
		2						200	1.1	0.17	23.56	0.7	43	28	29	0	0.1269	0.26
		3						1000	1.3	0.17	8.46	0.4	46	28	26	0	0.2265	0.26
CLVERTISOLS		1	D	1000	0.50	0.50	Sand	100.000	1.210	0.125	0.000	0.720	56.000	27.000	17.000	3.000	0.231	0.147
		2						200.000	1.400	0.056	4.960	0.700	23.000	45.000	32.000	0.000	0.127	0.348
		3						1000.000	1.400	0.056	4.530	0.400	25.000	36.000	38.000	0.000	0.227	0.348

Where: - NLAYERS Number of layers in the soil (min 1 max 3)

HYDGRP Soil hydrographic group (A, B, C, D)

SOL_ZMX Maximum root depth of the soil profile

ANION_EXCL Fraction of porosity from which an ions are exchanged

SOL_CRK Crack volume potential of soil

TEXTURE Texture of the layer

SOIL_Z Minimum depth from soil surface to bottom of layer

SOL_BD Moist bulk density

SOL_AWC Available water capacity of soil surface to bottom of the layer

SOL_K Saturated hydraulic conductivity

SOL_CBN Organic carbon content

CLAY Clay content

SILT Silt content

SAND Sand content

ROCK Rock fragmented content

SOL_ALB Moist soil albedo

USLE_K Soil erodibility factor (K)

Appendix 4 Annual average of sediment from each sub-basins

Sub-basin no.	1994 Sed in ton/ha/yr	2000 Sed. Yield in ton/ha/yr	2017Sed. yield In ton/ha/yr	Sub-basin no.	1994 Sed yield in ton/ha/yr	2000 Sed Yield in ton/ha/yr	2017 Sed. Yield In ton/ha/yr
1	9.2	10.5393	17.9035	144	27.8	29.7781	44.1459
2	22.0	24.26	34.6312	145	82.7	25.4929	52.5422
3	22.4	56.4634	74.6514	146	21.7	33.9826	51.0724
4	12.9	68.447	70.0301	147	5.8	11.6415	19.366
5	25.6	49.4499	54.827	148	6.6	11.3517	21.7655
6	14.3	24.0245	30.9367	149	18.5	15.0473	21.225
7	4.9	14.2444	21.3938	150	1.5	2.49821	5.64664
8	9.8	41.9669	46.4871	151	20.7	16.006	27.5048
9	2.2	2.29721	8.29893	152	21.4	17.6297	26.2076
10	3.3	3.56	7.75882	153	45.3	28.0352	21.434
11	2.3	0.52493	12.9505	154	19.8	2.25361	5.46464
12	3.2	1.74318	6.51154	155	108.8	94.6285	51.5585
13	3.0	3.95232	13.7604	156	9.5	14.7885	14.9134
14	29.8	47.6916	55.407	157	7.1	13.7515	17.9504
15	9.5	7.54493	10.7524	158	40.6	34.1556	46.645
16	40.6	45.076	72.4185	159	6.8	8.75225	14.6963
17	2.1	46.0987	64.0916	160	25.0	16.9722	24.9952
18	1.7	31.0641	49.2299	161	13.4	13.5148	18.3655
19	3.3	3.25689	10.7771	162	12.5	12.6767	17.6848
20	4.8	5.38146	7.67711	163	7.5	13.2378	24.3894
21	16.7	19.2699	35.4282	164	29.2	40.4051	12.6703
22	16.5	31.2801	42.667	165	4.4	10.2891	20.7453
23	13.0	12.6354	27.4245	166	3.5	5.13654	6.42271
24	3.5	3.97314	16.2667	167	3.8	3.6535	7.61096
25	1.3	3.52179	9.17321	168	17.7	15.6895	22.2923
26	0.4	3.11093	5.33629	169	5.0	3.12886	6.39771
27	11.7	18.6283	17.6508	170	3.7	3.37132	9.04061
28	10.2	39.3801	38.9952	171	5.2	9.88907	20.7298
29	15.4	38.2919	57.51	172	0.1	0.10325	1.91607
30	1.9	34.4649	45.099	173	4.9	2.05821	6.69321
31	17.2	41.5213	54.8138	174	40.3	10.8112	13.7026
32	1.4	29.0806	40.1236	175	48.1	11.7115	17.3386
33	1.3	19.6321	26.8154	176	6.8	12.4123	27.516

continued

34	65.2	63.4659	114.939	177	5.4	9.09139	19.614
35	19.9	20.0027	27.872	178	7.1	14.9517	23.994
36	5.6	4.71157	11.131	179	6.9	9.17464	24.0282
37	33.3	16.9487	60.5942	180	0.3	0.42254	1.24439
38	32.6	21.57	51.6978	181	1.3	1.70157	2.62739
39	9.3	9.0505	12.2839	182	4.9	7.61218	24.8426
40	34.6	13.3478	66.6292	183	1.7	1.12061	6.6975
41	56.7	42.8554	139.272	184	28.6	7.68386	10.9702
42	1.4	1.79896	6.80271	185	12.2	18.4179	23.5008
43	14.5	36.506	41.9693	186	3.2	5.55032	17.6615
44	0.2	39.6213	44.6935	187	14.0	14.7698	27.4545
45	2.6	4.61207	11.6402	188	9.2	8.71614	24.0599
46	2.6	1.49229	12.3616	189	10.2	10.9758	17.3367
47	1.0	4.22857	9.07121	190	2.5	3.17604	11.7787
48	0.2	1.39657	5.49325	191	7.4	5.44086	16.6327
49	39.1	25.7525	65.9782	192	3.6	3.40489	6.15525
50	21.7	20.7325	45.0813	193	6.7	13.8305	25.4649
51	9.0	16.5022	17.0815	194	3.9	5.223	7.68618
52	27.6	29.5519	33.6898	195	11.2	13.8785	31.9719
53	1.3	20.8091	31.3945	196	1.9	1.15904	4.76514
54	1.7	7.51143	15.1791	197	4.7	3.64993	14.7649
55	2.8	3.97321	9.52379	198	7.1	8.9725	19.9328
56	2.5	2.88282	6.94536	199	8.1	17.4006	32.8022
57	0.1	0.23089	2.45643	200	11.9	15.4449	31.2028
58	0.4	1.53582	7.79529	201	1.6	0.38229	5.24311
59	3.5	3.84071	14.9869	202	2.8	0.44568	6.17679
60	58.3	42.1133	127.747	203	7.6	11.829	21.5052
61	44.7	49.5106	157.576	204	1.3	1.34029	3.80936
62	4.7	3.12618	16.4703	205	10.0	14.271	29.9682
63	4.0	1.36546	6.83743	206	8.3	13.0606	36.0001
64	1.2	1.25964	14.4364	207	8.5	10.9	21.6913
65	12.0	26.4253	47.5679	208	19.7	6.53029	9.56136
66	0.9	22.7391	28.0789	209	0.7	0.74736	1.92546
67	5.9	11.499	11.286	210	12.1	16.4569	32.9153
68	5.9	4.237	10.807	211	11.0	9.19425	37.466
69	3.1	4.57871	16.0379	212	7.8	5.61793	23.0668
70	1.5	3.26929	9.64729	213	7.0	8.12471	20.4305
71	7.4	24.2498	31.453	214	7.2	8.72271	20.1868
72	6.4	7.39236	7.70639	215	12.5	2.46204	4.94386

continued

73	73.4	64.3124	148.404	216	19.2	7.12804	10.6524
74	18.2	33.0226	48.975	217	35.6	19.3982	10.2267
75	2.4	3.9475	13.5833	218	8.0	12.322	25.5339
76	12.0	9.90464	18.5194	219	7.3	3.95475	11.668
77	19.0	54.6792	80.2816	220	5.8	7.80711	19.214
78	11.9	20.0313	38.7392	221	10.2	3.41257	6.86711
79	17.1	36.6967	37.048	222	0.8	0.68321	2.0475
80	36.3	34.2127	35.4937	223	16.5	3.895	5.60268
81	58.6	81.0575	109.928	224	12.7	6.16329	4.34532
82	116.2	56.6631	162.484	225	9.1	6.80607	17.2307
83	3.5	8.79536	14.1679	226	5.7	10.1927	17.5613
84	1.2	1.55518	7.59575	227	1.9	1.63721	5.16232
85	0.9	2.65139	8.89393	228	8.7	2.58296	5.08071
86	0.6	0.84104	8.24671	229	3.0	2.67364	4.091
87	8.3	8.1735	20.3638	230	20.1	3.13239	6.4805
88	4.2	2.00196	11.1755	231	6.5	0.60625	1.60857
89	2.2	28.8649	41.0751	232	3.8	3.12329	5.51889
90	1.8	14.3999	23.1493	233	7.2	5.17614	10.1963
91	3.8	3.40532	12.1238	234	14.5	3.08579	5.15675
92	20.0	19.2048	30.988	235	0.7	0.80596	3.4895
93	12.0	13.2799	22.2663	236	4.6	3.76304	6.65075
94	0.4	0.58539	3.83186	237	6.3	6.90221	9.40414
95	12.2	12.1636	33.3255	238	5.2	1.211	5.10175
96	4.1	2.99261	8.24361	239	7.5	2.21893	4.08207
97	20.8	15.9776	53.754	240	6.5	6.37754	12.075
98	10.1	9.30257	33.5903	241	8.5	1.64746	4.44843
99	27.5	19.3629	29.9349	242	11.5	2.18779	4.37271
100	8.0	7.27832	15.4733	243	7.8	0.63246	1.643
101	9.9	20.7981	22.1003	244	0.5	0.48339	1.85143
102	7.4	12.041	26.2165	245	5.1	4.5	8.65236
103	12.9	17.8231	31.5875	246	0.7	0.81118	2.77618
104	27.6	17.3523	34.554	247	0.6	0.3885	2.72714
105	29.5	37.898	73.1368	248	1.6	1.3925	2.93604
106	25.1	28.616	50.3415	249	2.0	1.88614	3.24896
107	101.6	103.676	147.461	250	5.2	4.62	10.6089
108	0.8	0.50946	3.02118	251	2.8	2.30518	2.87432
109	21.3	24.6466	49.4233	252	10.1	1.49389	3.51479
110	99.0	111.561	128.542	253	0.7	0.61796	1.80336
111	50.0	34.2473	42.4228	254	0.9	0.87118	2.12579

continued

112	15.4	21.0571	33.8871	255	10.7	1.68604	1.02896
113	30.5	30.4108	49.4918	256	1.5	1.20389	2.19243
114	123.3	83.9748	135.462	257	7.0	6.60007	10.1071
115	54.3	31.0678	49.5931	258	2.0	1.95114	3.47679
116	75.0	51.975	79.9844	259	3.4	2.533	5.19721
117	13.1	15.2166	20.0576	260	0.5	0.489	2.33646
118	60.5	51.8363	90.58	261	0.6	0.54014	1.60364
119	17.5	13.1863	26.731	262	0.8	0.55971	3.61914
120	25.9	30.823	40.9891	263	9.1	0.53704	2.19639
121	129.0	71.8599	140.462	264	3.0	2.15236	2.84561
122	37.5	36.42	38.4651	265	23.9	15.6754	8.38339
123	11.8	10.6654	19.9051	266	4.4	3.05468	3.1455
124	18.9	16.3952	24.8268	267	66.2	44.182	26.5795
125	11.6	11.343	16.201	268	0.6	0.52429	1.70407
126	42.9	30.5958	39.4016	269	26.4	20.0713	15.742
127	31.7	23.4905	38.1728	270	51.6	44.602	21.7641
128	19.0	17.2999	27.7874	271	37.7	32.8908	20.915
129	6.8	9.068	16.6506	272	0.6	0.57229	1.56682
130	13.5	9.38932	19.302	273	53.2	47.0524	32.2779
131	1.1	0.69368	3.73229	274	0.8	2.21771	6.88946
132	0.5	0.36164	2.02504	275	0.5	0.44057	1.66825
133	17.2	17.1244	40.7386	276	24.2	22.309	13.6785
134	27.8	42.0092	61.5118	277	50.5	44.4283	27.8814
135	28.4	43.9718	58.3716	278	67.3	58.0319	27.7294
136	6.0	15.7829	32.1632	279	21.5	24.0263	12.8689
137	6.8	12.0945	32.7849	280	0.4	0.41704	1.19443
138	4.3	10.8315	36.5298	281	41.3	36.8504	23.092
139	1.6	0.94168	3.18693	282	13.9	12.8048	7.19407
140	0.6	0.68954	2.39618	283	20.5	15.7281	11.5124
141	18.2	14.4945	25.6095	284	41.8	39.5403	25.3142
142	19.2	18.2306	28.1563	285	26.8	22.8933	15.2268
143	26.2	38.5297	46.7695	286	36.1	33.4306	16.947

Appendix: 5 calibrated parameter for flow and sediment

calibrated flow parameter of 1994 model

Parameter_Name	Fitted_Value	Min_value	Max_value	unit	calibration value	remark
1:R__CN2.mgt	0.1275	0	0.2	na	vary	default is multiplied by fitted value within the allowable range
2:V__ALPHA_BF.gw	0.9675	0	1	[days]	0.9675	default is replaced by fitted value within the allowable range
3:V__GW_DELAY.gw	49.950001	30	450	[days]	49.950001	default is replaced by fitted value within the allowable range
4:V__GWQMN.gw	687.5	0	5000	[mm]	687.5	default is replaced by fitted value within the allowable range
5:V__EPCO.bsn	0.5375	0	1	na	0.5375	default is replaced by fitted value within the allowable range
6:R__HRU_SLP.hru	0.017	-0.2	0.2	[m/m]	vary	default is multiplied by fitted value within the allowable range
7:V__CANMX.hru	59.25	0	100	[mm]	59.25	default is replaced by fitted value within the allowable range
8:R__SOL_AWC(..).sol	-0.0695	-0.1	0.1	[mm/mm]	vary	default is multiplied by fitted value within the allowable range
9:R__SOL_K(..).sol	0.04325	0	0.1	[mm/hr]	vary	default is multiplied by fitted value within the allowable range
10:V__GW_REVAP.gw	0.11855	0.02	0.2	na	0.11855	default is replaced by fitted value within the allowable range
11:V__ESCO.hru	0.2725	0	1	na	0.2725	default is replaced by fitted value within the allowable range
12:V__CH_N2.rte	0.100625	0.01	0.3	na	0.100625	default is replaced by fitted value within the allowable range
13:R__SLSUBBSN.hru	-0.0556	-0.1	0.15	[m]	vary	default is multiplied by fitted value within the allowable range
14:R__SOL_Z(..).sol	0.0645	0	0.2	[mm]	vary	default is multiplied by fitted value within the allowable range
15:V__REVAPMN.gw	486.25	0	500	[mm]	486.25	default is replaced by fitted value within the allowable range
16:R__SOL_ALB(..).sol	0.00475	0	0.1	na	vary	default is multiplied by fitted value within the allowable range
17:V__SURLAG.bsn	2.385125	0.05	24	[days]	2.385125	default is replaced by fitted value within the allowable range
18:V__CH_K2.rte	67.875	0	150	[mm/hr]	67.875	default is replaced by fitted value within the allowable range
19:V__CH_K1.sub	200.25	0	300	[mm/hr]	200.25	default is replaced by fitted value within the allowable range
20:V__OV_N.hru	0.779725	0.01	1	na	0.779725	default is replaced by fitted value within the allowable range
21:V__RCHRG_DP.gw	0.1925	0	1	[fraction]	0.1925	default is replaced by fitted value within the allowable range

calibrated flow parameter of 2000 model

Parameter_Name	Fitted_Value	Min_value	Max_value	unit	calibration value	remark
1:R__CN2.mgt	0.02725	0	0.1	na	vary	default is multiplied by fitted value within the allowable range
2:V__ALPHA_BF.gw	0.7575	0	1	[days]	0.7575	default is replaced by fitted value within the allowable range
3:V__GW_DELAY.gw	140.25	30	450	[days]	140.25	default is replaced by fitted value within the allowable range
4:V__GWQMN.gw	312.5	0	5000	[mm]	312.5	default is replaced by fitted value within the allowable range
5:V__EPCO.bsn	0.0025	0	1	na	0.0025	default is replaced by fitted value within the allowable range
6:R__HRU_SLP.hru	0.117	-0.2	0.2	[m/m]	vary	default is multiplied by fitted value within the allowable range
7:V__CANMX.hru	87.75	0	100	[mm]	87.75	default is replaced by fitted value within the allowable range
8:R__SOL_AWC(..).sol	0.0545	-0.1	0.1	[mm/mm]	vary	default is multiplied by fitted value within the allowable range
9:R__SOL_K(..).sol	0.05875	0	0.1	[mm/hr]	vary	default is multiplied by fitted value within the allowable range
10:V__GW_REVAP.gw	0.17705	0.02	0.2	na	0.17705	default is replaced by fitted value within the allowable range
11:V__ESCO.hru	0.7475	0	1	na	0.7475	default is replaced by fitted value within the allowable range
12:V__CH_N2.rte	0.220975	0.01	0.3	na	0.220975	default is replaced by fitted value within the allowable range
13:R__SLSUBBSN.hru	0.075625	-0.1	0.15	[m]	vary	default is multiplied by fitted value within the allowable range
14:R__SOL_Z(..).sol	0.1985	0	0.2	[mm]	vary	default is multiplied by fitted value within the allowable range
15:V__REVAPMN.gw	111.25	0	500	[mm]	111.25	default is replaced by fitted value within the allowable range
16:R__SOL_ALB(..).sol	0.08525	0	0.1	na	vary	default is multiplied by fitted value within the allowable range
17:V__SURLAG.bsn	5.259125	0.05	24	[days]	5.259125	default is replaced by fitted value within the allowable range
18:V__CH_K2.rte	51.375	0	150	[mm/hr]	51.375	default is replaced by fitted value within the allowable range
19:V__CH_K1.sub	233.25	0	300	[mm/hr]	233.25	default is replaced by fitted value within the allowable range
20:V__OV_N.hru	0.819325	0.01	1	na	0.819325	default is replaced by fitted value within the allowable range
21:V__RCHRG_DP.gw	0.0625	0	1	[fraction]	0.0625	default is replaced by fitted value within the allowable range

calibrated flow parameter of 2017 model

Parameter_Name	Fitted_Value	Min_value	Max_value	unit	calibration value	remark
1:R__CN2.mgt	0.1275	0	0.2	na	vary	default is multiplied by fitted value within the allowable range
2:V__ALPHA_BF.gw	0.9675	0	1	[days]	0.9675	default is replaced by fitted value within the allowable range
3:V__GW_DELAY.gw	49.950001	30	450	[days]	49.95	default is replaced by fitted value within the allowable range
4:V__GWQMN.gw	687.5	0	5000	[mm]	687.5	default is replaced by fitted value within the allowable range
5:V__EPCO.bsn	0.5375	0	1	na	0.5375	default is replaced by fitted value within the allowable range
6:R__HRU_SLP.hru	0.017	-0.2	0.2	[m/m]	vary	default is multiplied by fitted value within the allowable range
7:V__CANMX.hru	59.25	0	100	[mm]	59.25	default is replaced by fitted value within the allowable range
8:R__SOL_AWC(..).sol	-0.0695	-0.1	0.1	[mm/mm]	vary	default is multiplied by fitted value within the allowable range
9:R__SOL_K(..).sol	0.04325	0	0.1	[mm/hr]	vary	default is multiplied by fitted value within the allowable range
10:V__GW_REVAP.gw	0.11855	0.02	0.2	na	0.11855	default is replaced by fitted value within the allowable range
11:V__ESCO.hru	0.2725	0	1	na	0.2725	default is replaced by fitted value within the allowable range
12:V__CH_N2.rte	0.100625	0.01	0.3	na	0.10063	default is replaced by fitted value within the allowable range
13:R__SLSUBBSN.hru	-0.0556	-0.1	0.15	[m]	vary	default is multiplied by fitted value within the allowable range
14:R__SOL_Z(..).sol	0.0645	0	0.2	[mm]	vary	default is multiplied by fitted value within the allowable range
15:V__REVAPMN.gw	486.25	0	500	[mm]	486.25	default is replaced by fitted value within the allowable range
16:R__SOL_ALB (...).sol	0.00475	0	0.1	na	vary	default is multiplied by fitted value within the allowable range
17:V__SURLAG.bsn	2.385125	0.05	24	[days]	2.38513	default is replaced by fitted value within the allowable range
18:V__CH_K2.rte	67.875	0	150	[mm/hr]	67.875	default is replaced by fitted value within the allowable range
19:V__CH_K1.sub	200.25	0	300	[mm/hr]	200.25	default is replaced by fitted value within the allowable range
20:V__OV_N.hru	0.779725	0.01	1	na	0.77973	default is replaced by fitted value within the allowable range
21:V__RCHRG_DP.gw	0.1925	0	1	[fraction]	0.1925	default is replaced by fitted value within the allowable range

calibrated sediment parameters 1994

Parameter_Name	value used in swat cup for calibration			unit	calibrated value	remark
	Fitted Value	Min value	Max value			
1:R__USLE_K(..).sol	0.003779	-0.002525	0.005825	na	vary	default is multiplied by fitted value within the allowable range
2:V__CH_N2.rte	0.045224	0.014876	0.04699	na	0.045224	default is replaced by fitted value within the allowable range
3:V__EPCO.hru	0.563181	0.454272	0.563728	na	0.563181	default is replaced by fitted value within the allowable range
4:R__SOL_Z(..).sol	0.057125	0.008479	0.149483	[mm]	vary	default is multiplied by fitted value within the allowable range
5:V__ESCO.hru	0.985271	0.579161	1	na	0.985271	default is replaced by fitted value within the allowable range
6:V__ALPHA_BF.gw	0.598586	0.47619	0.87749	[days]	0.598586	default is replaced by fitted value within the allowable range
7:V__SPCON.bsn	0.000955	0.0001	0.006	na	0.000955	default is replaced by fitted value within the allowable range
8:V__CH_K2.rte	379.48987	280.15115	447.10696	[mm/hr]	379.489868	default is replaced by fitted value within the allowable range
9:R__USLE_P.mgt	0.0175	0	0.5	na	vary	default is multiplied by fitted value within the allowable range
10:V__SPEXP.bsn	1.314028	1.140279	1.318483	na	1.314028	default is replaced by fitted value within the allowable range
11:R__SLSUBBSN.hru	0.009457	0.004009	0.159675	[m]	0.009457	default is replaced by fitted value within the allowable range
12:V__SURLAG.bsn	22.813086	14.666316	24.1947	[days]	22.813086	default is replaced by fitted value within the allowable range
13:R__SOL_AWC(..).sol	0.038757	0.03012	0.131726	[mm/mm]	vary	default is multiplied by fitted value within the allowable range
14:R__SLSOIL.hru	-0.1594	-0.172	-0.022	[m]	vary	default is multiplied by fitted value within the allowable range
15:R__SOL_K(..).sol	-0.19	-0.2	0.2	[mm/hr]	vary	default is multiplied by fitted value within the allowable range
16:V__CH_COV1.rte	0.97222	0.707584	1	na	0.97222	default is replaced by fitted value within the allowable range
17:V__CH_COV2.rte	0.724236	0.533617	0.727139	na	0.724236	default is replaced by fitted value within the allowable range
18:V__CANMX.hru	75.800003	60	100	[mm]	75.800003	default is replaced by fitted value within the allowable range
19:R__CN2.mgt	0.248752	0.166787	0.25	na	vary	default is multiplied by fitted value within the allowable range
20:R__FFCB.bsn	0.215	0	1	[fraction]	vary	default is multiplied by fitted value within the allowable range
21:R__RSDCO.bsn	0.084188	0.057444	0.109374	na	vary	default is multiplied by fitted value within the allowable range

Where R: relative to default and V is replacing of default

calibrated sediment parameter of 2000

Parameter Name	value used in swat cup				calibration value	remark
	Fitted Value	Min value	Max value	unit		
1:R__USLE_K(..).sol	-0.1947	-0.2	0.01	na	vary	default is multiplied by fitted value within the allowable range
2:V__CH_N2.rte	0.0433	0.01	0.3	na	0.04335	default is replaced by fitted value within the allowable range
3:V__EPCO.hru	0.4789	0.37	0.55	na	0.4789	default is replaced by fitted value within the allowable range
4:R__SOL_Z(..).sol	0.09813	0.072353	0.219647	[mm]	vary	default is multiplied by fitted value within the allowable range
5:V__ESCO.hru	0.742289	0.29139	0.888607	na	0.74229	default is replaced by fitted value within the allowable range
6:V__ALPHA_BF.gw	0.2286	-0.020	0.6628	[days]	0.22869	default is replaced by fitted value within the allowable range
7:V__SPCON.bsn	0.003847	0.0001	0.006	na	0.00385	default is replaced by fitted value within the allowable range
8:V__CH_K2.rte	144.15338	109.5415	332.843903	[mm/hr]	144.153	default is replaced by fitted value within the allowable range
9:R__USLE_P.mgt	0.0475	0	0.5	na	vary	default is multiplied by fitted value within the allowable range
10:V__SPEXP.bsn	1.4975	1	1.5	na	1.4975	default is replaced by fitted value within the allowable range
11:R__SLSUBBSN.hru	0.140774	0.07786	0.237135	[m]	0.14077	default is replaced by fitted value within the allowable range
12:V__SURLAG.bsn	14.719808	7.998302	24.1947	[days]	14.7198	default is replaced by fitted value within the allowable range
13:R__SOL_AWC(..).sol	0.155	0	0.2	[mm/mm]	vary	default is multiplied by fitted value within the allowable range
14:R__SLSOIL.hru	-0.0762	-0.2	0.05	[m]	vary	default is multiplied by fitted value within the allowable range
15:R__SOL_K(..).sol	0.19	-0.2	0.2	[mm/hr]	vary	default is multiplied by fitted value within the allowable range
16:V__CH_COV1.rte	0.445865	0.199443	0.505557	na	0.44587	default is replaced by fitted value within the allowable range
17:V__CH_COV2.rte	0.435565	0.001	1	na	0.43557	default is replaced by fitted value within the allowable range
18:V__CANMX.hru	99.800003	60	100	[mm]	99.8	default is replaced by fitted value within the allowable range
19:R__CN2.mgt	-0.1425	-0.25	0.25	na	vary	default is multiplied by fitted value within the allowable range
20:R__FFCB.bsn	0.025	0	1	[fraction]	vary	default is multiplied by fitted value within the allowable range
21:R__RSDCO.bsn	0.0596	0.02	0.1	na	vary	default is multiplied by fitted value within the allowable range

Where R: relative to default and V is replacing of default

calibrated sediment parameters 2017

Parameter Name	value used in swat cup			unit	calibrated value	Remark
	Fitted Value	Min value	Max value			
1:R__CN2.mgt	-0.19195	-0.25	0.02	na	vary	default is multiplied by fitted value within the allowable range
2:V__ALPHA_BF.gw	0.5715	0.3	0.6	[days]	0.5715	default is replaced by fitted value within the allowable range
3:V__SPCON.bsn	0.042316	0.000266	0.06864	na	0.04232	default is replaced by fitted value within the allowable range
4:V__CH_N2.rte	0.12375	0.1	0.29	na	0.12375	default is replaced by fitted value within the allowable range
5:V__CH_K2.rte	402.00501	83	500	[mm/hr]	402.005	default is replaced by fitted value within the allowable range
6:R__USLE_P.mgt	0.538488	0.06662	0.7	na	vary	default is multiplied by fitted value within the allowable range
7:V__SPEXP.bsn	1.487281	1.232486	1.7	na	1.48728	default is replaced by fitted value within the allowable range
8:V__CANMX.hru	63.975002	45	100	[mm]	63.975	default is replaced by fitted value within the allowable range
9:R__SLSUBBSN.hru	-0.077264	-0.12161	0.075471	[m]	vary	default is multiplied by fitted value within the allowable range
10:V__SURLAG.bsn	18.605	11	24	[days]	18.605	default is replaced by fitted value within the allowable range
11:V__EPCO.hru	0.2296	0.06	0.7	na	0.2296	default is replaced by fitted value within the allowable range
12:V__ESCO.hru	0.252799	-0.1848	0.618132	na	0.2528	default is replaced by fitted value within the allowable range
13:R__SOL_AWC(..).sol	0.100287	-0.04646	0.25	[mm/mm]	vary	default is multiplied by fitted value within the allowable range
14:R__SOL_Z(..).sol	-0.0665	-0.19	0.07	[mm]	vary	default is multiplied by fitted value within the allowable range
15:R__SLSOIL.hru	0.1555	-0.05	0.25	[m]	vary	default is multiplied by fitted value within the allowable range
16:R__SOL_K(..).sol	0.059525	-0.0136	0.162604	[mm/hr]	vary	default is multiplied by fitted value within the allowable range
17:V__CH_COV1.rte	0.44325	0.05	0.6	na	0.44325	default is replaced by fitted value within the allowable range
18:V__CH_COV2.rte	0.8605	0.1	1	na	0.8605	default is replaced by fitted value within the allowable range
19:R__USLE_K(..).sol	-0.187	-0.2	0	na	vary	default is multiplied by fitted value within the allowable range

Where R: relative to default and V is replacing of default